

**INVESTIGATION ON EMISSION FEATURES OF
TTBC AGGREGATES IN PVA FIBER MATS BY
ELECTROSPINNING**

**A Thesis Submitted to
the Graduate School of Engineering and Sciences of
İzmir Institute of Technology
in Partial Fulfillment of the Requirements for the Degree of**

MASTER OF SCIENCE

in Chemistry

**by
Bengisu ÖZEN**

**July 2010
İZMİR**

We approve the thesis of **Bengisu ÖZEN**

Assist. Prof. Mustafa M. DEMİR
Supervisor

Prof. Serdar ÖZÇELİK
Co-Supervisor

Assist. Prof. Nuran ELMACI
Committee Member

Assist. Prof. M. Salih DİNLEYİCİ
Committee Member

Assist. Prof. Canan VARLIKLI
Committee Member

12 July 2010

Prof. Serdar ÖZÇELİK
Head of the Department of Chemistry

Assoc. Prof. Talat YALÇIN
Dean of the Graduate School of
Engineering and Science

ABSTRACT

INVESTIGATION ON EMISSION FEATURES OF TTBC AGGREGATES IN PVA FIBER MATS BY ELECTROSPINNING

1,1',3,3'-tetraethyl-5,5',6,6'-tetrachlorobenzimidazolocarbo-cyanine (TTBC) is a frequently used cyanine dye that undergoes two different types of molecular aggregate (J and H-type). Dye molecules, in general, come into aggregation in ionic solutions and solid surfaces without control over the type and orientation of the resulting aggregate. In this research, we focused on electrospinning of aqueous poly(vinyl alcohol) (PVA)/TTBC solutions and investigated whether the aggregate formation could be controlled by solution and instrumental parameters of this process. Initially, TTBC was molecularly dispersed in aqueous PVA solution with a weight fraction of 0.001- 0.65 % and the precursor solution was subjected to electrospinning under electrical field ranging from 0.95-1.81 kV/cm. A stationary horizontal electrospinning set-up was used including two parallel-positioned metal strips as counter electrode. Both randomly-deposited and uniaxially aligned fibers were achieved. For the reason of comparison, reference films were prepared by spin-coating and film casting. Photoluminescence and polarized FTIR spectroscopy techniques were employed to examine spectral properties of the fibers. While H- and J-type aggregates coexist within spin-coated films and only J-aggregates exist within cast films, only H-type aggregates were observed within the fibers regardless of their alignment. A strong polarized emission was obtained from the uniaxially aligned fibers due to the orientation of H-aggregates along the fibers. Consequently, electrospinning was found to be an alternative method to bring individually dispersed dye molecules into oriented H-type aggregates within submicron diameter fibers. Similar experimentation was also applied to TTBC/PS and Pyrene/Polystyrene(PS) systems to investigate aggregation behavior of dye molecules. TTBC exhibited similar behavior in PS/Dimethylformamide (DMF) system observed in PVA/H₂O system. However, electrospinning has no remarkable influence on aggregation of pyrene in excimers. It slightly disassemble excimer structure.

ÖZET

TTBC BOYA MOLEKÜLLERİNİN ELEKTRODOKUMA PVA LİFLERİ İÇERİSİNDEKİ İŞİMA ÖZELLİKLERİNİN İNCELENMESİ

1,1',3,3'-tetraetil-5,5',6,6'-tetraklorobenzimidazolokarbosyanin (TTBC) iki tip öbeklenme (J ve H-tipi) gösteren bir sayanın boyasıdır. Boya molekülleri genelde iyonik çözeltilerde ve katı yüzeylerde öbeklenme göstermektedir. Fakat bu öbeklerin çeşidini ve yönelimini kontrol etmek oldukça güçtür. Bu çalışmada, TTBC boyasını polivinil alkol (PVA) ile birlikte elektrodokuma yöntemine tabi tutularak, boyanın oluşturacağı öbeklenmelerin çeşidini ve yönelimini kontrol etmek hedeflenmiştir. Sulu PVA çözeltisi içerisinde monomerik halde dağıtılan TTBC molekülleri (kütlece %0,001 ile 0,65 oranında), kuvvetli elektrik alanı uygulanarak (0.95 ile 1.81 kV/cm), elektrodokuma işlemine tabi tutulmuştur. Yatay olarak tasarlanan elektrodokuma düzeneğinde, elektrot olarak birbirine paralel keskin uçlu iki metal levha kullanılmıştır. Oluşturulan lif yapılı filmlerin rastgele dağılmış ve yönlenmiş olmak üzere iki çeşit dizilişe sahip olduğu taramalı elektron mikroskopu ile saptanmıştır. Bunlara ek olarak, döngü kaplama ve dökme film adı verilen farklı iki ince film hazırlama tekniği de kullanılmış ve elektrodokumanın etkisi bu tekniklerle kıyaslanmıştır. TTBC boya molekülleri ve PVA'nın lif içerisindeki yapısal durumunu incelemek üzere sırasıyla fotoluminesans ve FTIR spektroskopisi kullanılmıştır. Döngü kaplama örnekler H- ve J-tipi, dökme film örnekleri sadece J-tipi öbeklenme gösterirken, elektrodokuma filmler sadece H-tipi öbeklenme göstermiştir. Fakat elektrodokuma liflerden yönlenmiş olan örnekler yüksek polarize özellik göstermiştir. İşimada gözlemlenen polarizasyonun sebebi ise H-öbeklerinin fiber yönünde yönlenmesidir. Sonuç olarak, elektrodokuma yönteminin lif yönünde H-tipi öbeklenme oluşturmada etkili bir yöntem olduğu anlaşılmıştır. TTBC/PVA sistemine ek olarak benzer deneyler TTBC/Polistiren(PS) ve Piren/PS sistemleri için de gerçekleştirilmiştir. Fakat elektrodokuma yöntemi, TTBC/PS sisteminde farklı bir etki göstermezken, Piren/PS sistemi için öbeklenmeye neden olmamıştır.

TABLE OF CONTENTS

TABLE OF CONTENTS.....	vi
LIST OF FIGURES	viii
LIST OF TABLES	xi
CHAPTER 1. INTRODUCTION	1
1.1. Electrospinning	1
1.2. Self-assembly.....	4
1.2.1. Molecular Dye Aggregates	4
1.3. Combination of Self-assembly and Electrospinning	8
CHAPTER 2. EXPERIMENTAL STUDY	10
2.1. Materials	10
2.2. Experimental.....	10
2.2.1. Preparation of Precursor Solutions	10
2.2.2. Preparation of Electrospun Films	11
2.2.3. Preparation of Spincoated Films.....	12
2.2.4. Preparation of Cast Films	12
2.3. Characterization of Samples	13
2.3.1. Scanning Electron Microscopy	13
2.3.2. Polarized Fourier Transform Infrared Spectroscopy	13
2.3.3. Photoluminescence Spectroscopy	14
2.3.4. UV-Visible Spectroscopy	14
CHAPTER 3. RESULTS AND DISCUSSIONS	15
3.1. Electrospinning of PVA Solution	15
3.2. Electrospinnig of TTBC Monomer/ PVA Solution	19
3.2.1. The Effect of [TTBC] on Molecular Aggregation.....	20
3.2.2. The Effect of Potential Difference on Molecular Aggregation	22
3.2.3. The Effect of Fiber Diameter on Molecular Aggregation	26

3.3. Electrospinning of J-aggregated TTBC	28
3.3.1. In the Absence of Polymer	28
3.3.2. In the Presence of Polymer	31
3.4. Comparison of Electrospun Mats with Spincoated and Cast Films.....	32
3.5. TTBC Doped PS Fibers	34
3.6. Pyrene Doped PS Fibers	35
CHAPTER 4. CONCLUSION	39
REFERENCES	40

LIST OF FIGURES

<u>Figure</u>	<u>Page</u>
Figure 1.1. Schematic representation of electrospinning set-up	1
Figure 1.2. The effect of polymer concentration on fiber diameter	3
Figure 1.3. Schematic representation of aggregate formation from monomers	5
Figure 1.4. Chemical structure of cyanine dyes	5
Figure 1.5. a) Schematic representation of dye molecules that form an aggregate (Source:(Emerson, et al. 1967), b) Absorption spectrum of TTBC dye in solution with diferent salt concentrations. M for monomer band, H and J for the blue-shifted and red-shifted H- and J-band, respectively (Source: Birkan, et al. 2006).....	6
Figure 1.6. Energy-band diagram of cyanine dye aggregates	7
Figure 1.7. Arrangement of dye molecules in J-aggregate [a) brickstone work, b) 30°-spaced agggregate, c) X-ray crystal structure model, d) Herringbone model] and e) H-aggregate structure (Source: Möhwald, et al. 1993).....	7
Figure 1.8. Molecular structure of a) Pseudoisocyanine-Bromide (PIC-Br), b) 1,1',3,3'-tetraethyl-5,5',6,6'-tetrachlorobenzimidazolocarboyanine-Iodide (TTBC)	8
Figure 2.1. Schematic representation of spincoating process	12
Figure 2.2. Schematic representation of cast film preparation.....	13
Figure 2.3. Schematic representation of polarized emission spectrometer	14
Figure 3.1. Electrical field lines between tip of the needle and collector in electrospinning process (a) a plate-like electrode that results in randomly deposited fibers, (b) a pair of parallel-positioned metal strips seperated with an air gap to fabricate uniaxially aligned fiber between two strips (Source: Li, et al. 2003).....	16
Figure 3.2. SEM micrograph of a) electrode and the e-spun fibers, b) randomly deposited PVA fibers collected on the surface of collector, c) uniaxially alligned fibers across the void gap	16
Figure 3.3. Histogram of the angle (θ) between the long axis of fibers and the normal of the long edge of the metal electrodes	17
Figure 3.4. Polarized FTIR spectra of a) randomly deposited, b) alligned PVA fibers that electrospun at 1.6 kV/cm, c) macroscopic alignment of e-spun fibers and monomeric residue of PVA.	18
Figure 3.5. PL spectra of electrospun PVA fibers.....	19
Figure 3.6. Absorption spectra of TTBC methanol solution at different concentrations	19

Figure 3.7. Average fiber diameters at different [TTBC]	21
Figure 3.8. a) PL spectrum of TTBC/PVA randomly deposited fibers, b) Aligned fibers prepared at different [TTBC] (excitation wavelength: 450nm).....	22
Figure 3.9. PL spectrum of a) randomly-deposited, b) Aligned fibers e-spun from 0.5 mM TTBC/PVA 10% at different potential differences	23
Figure 3.10. FTIR polarization graph of TTBC within PVA fibers.....	24
Figure 3.11. Polarized PL spectrum of a) aligned and b) random fibers of TTBC/PVA system performed at four different polarizer combination which are vertical-vertical, vertical-horizontal, horizontal-horizontal and horizontal-vertical with respect to the aligned fibers of 0.5 mM TTBC/PVA(10 wt%) prepared at 12.7kV.	25
Figure 3.12. Cartoon demonstration of aggregates within fibers (A crosssectional view).....	25
Figure 3.13. Polarized microscope images of aligned fibers performed at different polarization angles (the fibers prepared from 0.5 mM TTBC/PVA solution at 12.7 kV).....	26
Figure 3.14. Average fiber diameters versus PVA fraction	27
Figure 3.15. PL spectrum of electrospun fibers prepared at different PVA content (7.5- 10.0- 12.5- 15.0 wt %).....	27
Figure 3.16. The PL spectra of J-aggregated TTBC solution	28
Figure 3.17. SEM images of resultant sample which were electrospun from J-aggregated solution of TTBC at 1500, 10000, 35000× magnifications, respectively.....	29
Figure 3.18. The PL spectra of electrospun TTBC sample	29
Figure 3.19. a) Molecular structure of TDBC b) The PL spectra of TDBC J-aggregates.....	30
Figure 3.20. SEM images of electrospun TDBC sample at different magnifications (2500, 6500, 35000×, respectively)	31
Figure 3.21. PL spectra of electrospun TDBC samples	31
Figure 3.22. The emission spectra of a) J-aggregated TTBC in PVA solution, b) TTBC/PVA fibers electrospun from J-aaggregated solution.....	32
Figure 3.23. The photograph of a) electrospun, b) spincoated and c) cast film samples of TTBC/PVA solution.....	32
Figure 3.24. PL spectrum of A) Spincoated films prepared at different rotation speed, B) Cast film of TTBC(0.5 mM) /PVA (10 wt%).....	33
Figure 3.25. PL spectrum of TTBC/PVA thin film samples prepared by different film preparation techniques: Film casting, spincoating and electrospinning	34
Figure 3.26. PL spectra of 1mM TTBC/PS(25 wt%) solution.....	34

Figure 3.27. a) SEM image, b) PL spectra of TTBC/PS electrospun fibers	35
Figure 3.28. Molecular structure of Pyrene	35
Figure 3.29. PL spectrum of Py/PS solutions at different [Py]	36
Figure 3.30. SEM Images of a) 10^{-3} mM pyrene doped 25 wt% PS fibers, b) PS fiber surface (magnification at 20,000 \times)	36
Figure 3.31. PL spectra of Py/PS a) electrospun fibers, b) spincoated, c) cast films	37

LIST OF TABLES

<u>Table</u>	<u>Page</u>
Table 2.1. TTBC/ PVA contents in their solutions	10
Table 2.2. a) Instrumental parameters and optimizations of electrospinning process,.....	11
Table 3.1. SEM micrograph of a) aligned and b) randomly deposited fibers electrospun from %10 PVA solution at different [TTBC] (magnifications at 10,000×)	20
Table 3.2. SEM micrographs of aligned and random PVA/TTBC electrospun fibers at constant [TTBC] but different PVA content	26

CHAPTER 1

INTRODUCTION

1.1. Electrospinning

Electrospinning is a top-down approach that is highly ascendent method to generate continuous fibers where diameter can be controlled from a few nanometers to micrometers (Dzenis 2004). This method has able to produce polymeric, ceramic and composite fibers. The process was first patented by Formhals in 1934 (U.S. patent 1,975,504) and many investigations in electrospinning have been carried out by a number of researcher groups (Baumgarten 1971; Chen, et al. 2001; Fong, et al. 1999; Huang, et al. 2003; Li, et al. 2003; Reneker, et al. 1996; Yang, et al. 2005) and etc.).

Electrospinning in general consists of a syringe with a needle, an electrically conductive collector or electrode, and a DC power supply that produces potential difference on the order of tens of kV (Figure 1.1).

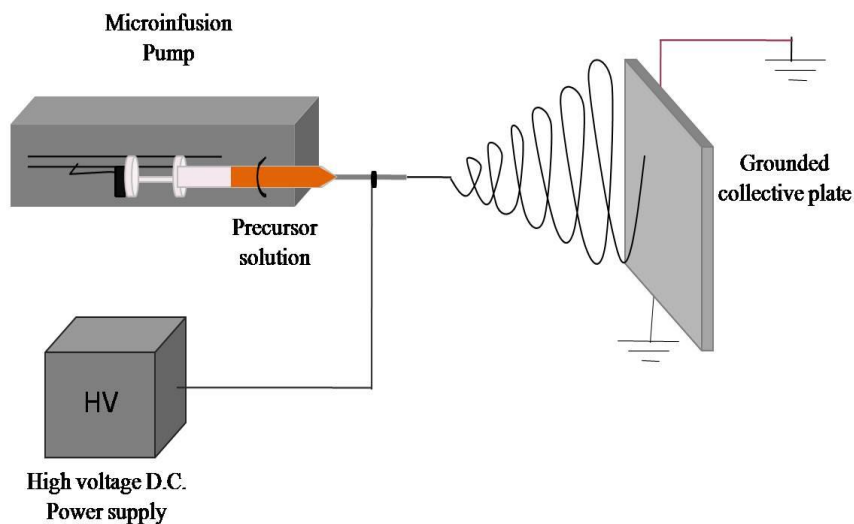


Figure 1.1. Schmatic representation of electrospinning set-up

The process starts with loading the precursor solution to a syringe. While the solution is pumping through the syringe needle at a specific flow rate which is set by a syringe pump, the electrical field is applied on the order of several kV. Electrical field causes deformation of the polymer droplet at the tip of the needle from hemispherical to

conical shape and this shape is called as Taylor cone (Taylor 1964). The electric field at the surface of the liquid produces a force and when the accumulated charge on the droplet surface overcomes the surface tension, a polymer jet emerges from the deformed droplet. Although the jet is stable near to the tip of the spinneret, it soon undergoes a bending instability stage because it begins to stretch and whip around due to the electrostatic interactions (Reneker, et al. 1996). Then, the solvent evaporates simultaneously with further stretching of the jet so the jet diameter becomes smaller. The charge on the jet tends to expand it in the radial directions and stretch in the axial direction. As the radius of the jet becomes smaller, the radial forces from the charge can become large enough to overcome the cohesive forces of the fiber and cause it to split into two or more fibres, that is to splay. This jet division process occurs several more times in rapid succession and produces a large number of small electrically charged fibres moving toward the collector. Finally, solid fibers are precipitated on the grounded collector.

Although the implementation of electrospinning process seems quite simple, understanding the physical rules behind the process is very complex because it includes many physical instability processes. While the jet travelling toward the charged substrate, it undergoes a series of instabilities (Reneker, et al. 2000). There are three different instabilities, namely Rayleigh, axisymmetric-conducting and bending-conducting instability during electrospinning process. Careful control of these instabilities ensures successful fiber formation. The axisymmetric Plateau-Rayleigh instability caused by the existence of tiny perturbations in the liquid stream and it causes beaded fiber formation. Electrospinning process also includes the off-axis bending instability that is largely responsible for the narrow fiber diameter. The bending instability is an essential part in the electrospinning process to elongate the jet and form the nanofibers.

The morphology of electrospun fibers depends on many parameters which can be divided into solution and instrumental parameters. Solution parameters are viscosity including concentration of solution and molecular weight of polymer, surface tension and electrical conductivity. Instrumental parameters are flow rate of the polymer solution, the field strength and geometry of the nozzle (Huang, et al. 2003). The dominant parameter is viscosity. In Figure 1.2, the effect of concentration on fiber diameter is shown. As viscosity of the polymer solution increase, the fiber diameter are increase exponentially.

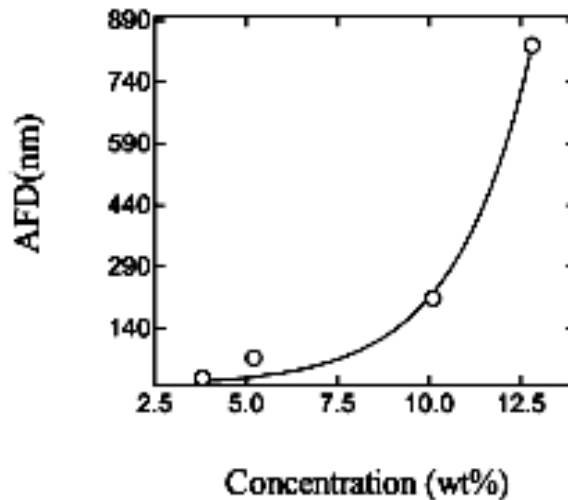


Figure 1.2. The effect of polymer concentration on fiber diameter
(Source: (Demir, et al. 2002))

The electrospun fibers have many advantages over fibers produced by conventional spinning. The most important advantage is providing high surface area to volume ratio. For instance, electrospinning of one gram of polymer solution yields nanofibers that have over 20 m² specific surface area (Deitzel, et al. 2002). The porosity and integrity are also the benefits of electrospun fibers. Moreover, electrospinning is an easy, low cost and fast process. Most importantly it provides template of nanostructures.

Great interest to electrospun fibers also caused by broad application areas such as in medical for wound dressing, also in textile industry for functional clothing, and in many others including energy, protective materials, agriculture, filtration and automotive industries.

The fibers that are produced by electrospinning are usually deposited on the collector as a non-woven mat, that means fibers have completely random orientation. Although these mats have many applications, their disordered structures seem to be problematic for device fabrications (in, for example, microelectronics and photonics) it is often required well aligned and highly ordered architectures. Therefore, there are several techniques that have been developed to organize the electrospun fibers into aligned arrays. For example, electrospinning with the help of a rotating mandrel (Moon, et al. 2008; Sundaray, et al. 2004), rotating disk (Theron, et al. 2001), frame electrode (Dersch, et al. 2003), scanning tip (Kameoka, et al. 2003) or wire drum (Katta, et al. 2004), parallel grounded conductive collectors (Li, et al. 2003) are the methods to achieve macroscopically aligned nanofibers. In addition, Kakade et al. used parallel

grounded conductive collectors during electrospinning and they have shown that electrospun fibers are not only macroscopically but also microscopically aligned because the polymer chains are oriented along the fiber axis. They have confirmed the molecular orientation via polarized FTIR, polarized Raman and X-ray diffraction (Kakade, et al. 2007).

1.2. Self-assembly

Self assembly is formation of complex structures of molecules or macromolecules via non-covalent molecular interactions. It is also commonly used as bottom-up approach in nanoscience and nanotechnology.

This process spontaneously creates significantly ordered structures from disordered components (Palmer, et al. 2008). These components must be able to move with respect to one another, means that they should be mobile and the interactions between the components are noncovalent such as Van der Waals, electrostatic, or hydrophobic interactions, hydrogen or coordination bonds. In self-assembly of larger components— meso- or macroscopic objects—interactions can include gravitational attraction, external electromagnetic fields, and magnetic, capillary, and entropic interactions which are not important in the case of molecules (Whitesides, et al. 1994).

Self-assembly is mechanistically divided into two categories which are static and dynamic ones (Whitesides, et al. 2002). In dynamic self-assembly the interactions that are responsible for the formation of structures or patterns between components only occur if the system dissipates energy. It means that the system requires an external energy to assemble and it is a non-equilibrium process. In formation of static self-assembly formation of the ordered structure may require energy, but once it is formed, it is an equilibrium process. Static self-assembly corresponds to what most chemists have been recognize as molecular self-assembly.

1.2.1. Molecular Dye Aggregates

Molecular aggregates are mesoscopic clusters of molecules, with sizes intermediate between crystals and isolated molecules. They belong to the group of nanostructure materials (Yamamoto, et al. 1993), which currently create much interest.

Among various functional molecules, dyes have become important materials in certain areas of nanotechnology. Although dye stuffs were previously used only for coloring, application of functional dyes to electronics, optoelectronics, and photonics has started to attract researchers' interest in the past decade and their aggregation behaviors have been actively studied. Concentrated aqueous or salt added dye solutions (Emerson, et al. 1967), solid or liquid interfaces (Yao, et al. 1999) also vertical spin-coating (Kobayashi, et al. 1997) result in the formation of aggregates from individually dispersed molecules (Figure 1.3). In addition, electrospinning is investigated in this study for this purpose.

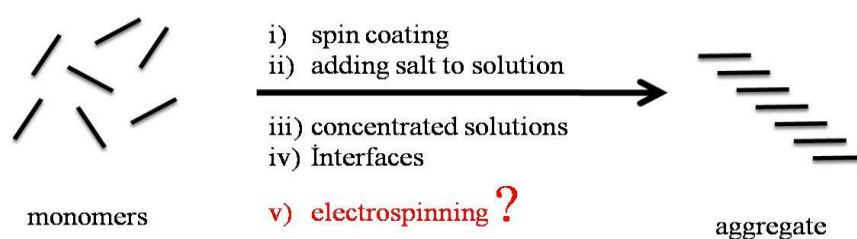


Figure 1.3. Schematic representation of aggregate formation from monomers

The best known aggregated organic dyes are cyanine dyes (Okamoto, et al. 2009). They have large dipole strength and therefore sharp absorption bands (Platt 1956). These dyes mainly have two nitrogen atoms that are each independently a part of at least two different heteroaromatic rings. The heteroaromatic rings are joined by a polymethine chain, which comprises a carbocyclic ring that is centrally located within the polymethine chain (Figure 1.4). The carbocyclic ring is derivatized with a hydrocarbyl or a substituted hydrocarbyl group at the meso position in a manner such that the dye is substantially fluorescent.

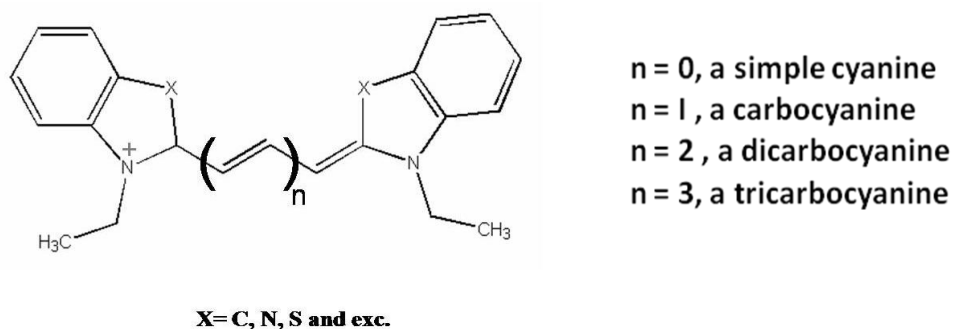


Figure 1.4. Chemical structure of cyanine dyes
(Source: Brooker, et al. 1951)

There is a great deal of confusion in the literature about the behavior of cyanine dyes, since they form very tightly bound aggregates and exhibit spectral shifts of the order of 100 nm as the aggregates form (James, et al. 1977). There are mainly two types of aggregates: H and J type. In Figure 1.5a, the oval shapes represent individual dye molecules called also monomers that form aggregate, the arrows represent the transition dipole moments of them and the line with an angle shows the aggregate axis. The angle between the aggregate axis and the transition dipole moments determines whether the aggregate is J or H type. The angle between 0 to 54°, a red shifted band is observed in the absorption spectrum which named as J band and for 54 to 90°, a blue shifted band observed which is called H-band (Figure 1.5b).

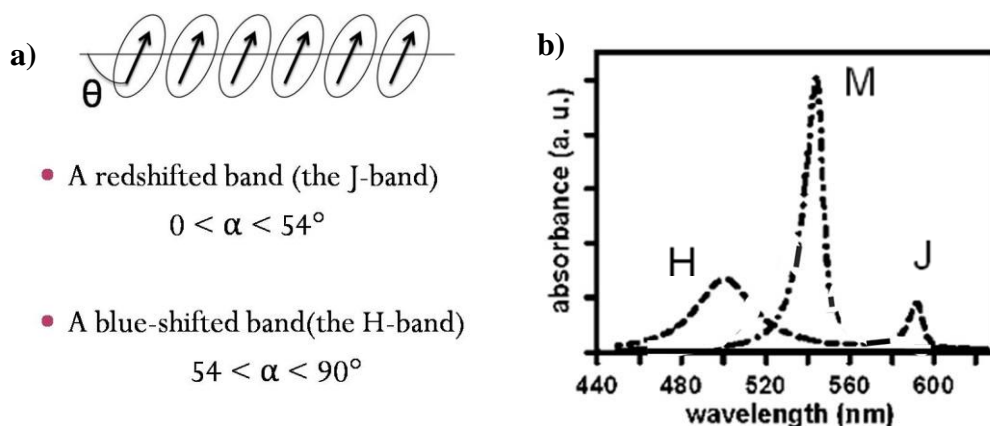


Figure 1.5. a) Schematic representation of dye molecules that form an aggregate (Source: Emerson, et al. 1967), b) Absorption spectrum of TTBC dye in solution with different salt concentrations. M for monomer band, H and J for the blue-shifted and red-shifted H- and J-band, respectively (Source: Birkan, et al. 2006)

The strong optical response of aggregates originates from collective effects of constituent molecules. This collective effect causes the strong interactions between the molecules that form aggregate. Therefore, the electronic states over molecules in the aggregate delocalize and the excitonic states form (Fidder, et al. 1995). The resultant absorption bands of these aggregates are explained in terms of molecular exciton theory. According to exciton theory, the dye molecule is regarded as a point dipole and the excitonic state of the dye aggregate splits into two levels through the interaction of transition dipoles. The dye molecules may aggregate in a parallel way (plane-to plane stacking) to form a sandwich-type arrangement (H-dimer) or in a head-to-tail arrangement (end-to end stacking) to form a J-dimer. A transition to the upper state in

parallel aggregates having parallel transition moments and to a lower state in a head-to-tail arrangement with perpendicular transition moments leading to hypsochromic (red) and bathochromic (blue) shifts, respectively (Figure 1.6).

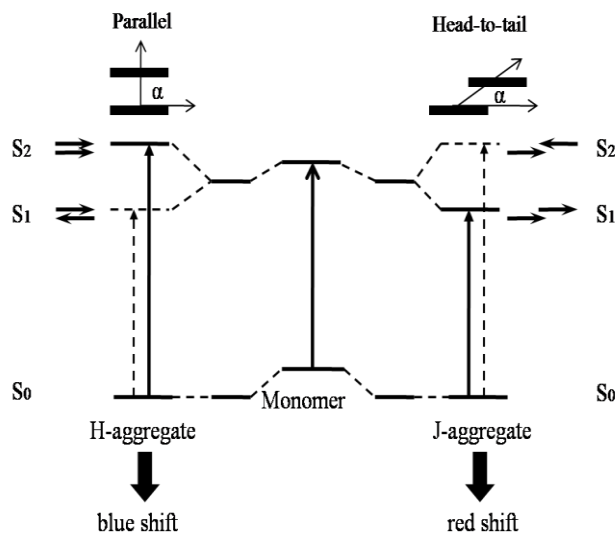


Figure 1.6. Energy-band diagram of cyanine dye aggregates (Source: Kasha 1959)

For geometrical arrangements for dye molecules, theoretical descriptions are used. Molecular arrangements of dye molecules in an aggregate as shown in Figure 1.7, can be in close-packed monolayers (O'Brien 1974), Scheibe ladder (Tani 1996) or staircase arrangements and variations including the brickstone-work arrangement (Kuhn 1970) suggested recently by Kuhn and co-workers, and the herringbone arrangement suggested by Bird and co-workers (Bird 1968).

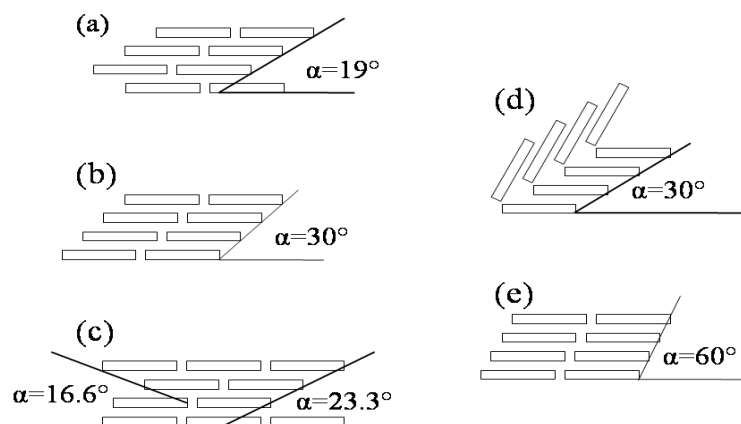


Figure 1.7. Arrangement of dye molecules in J-aggregate [a) brickstone work, b) 30°-spaced aggregate, c) X-ray crystal structure model, d) Herringbone model] and e) H-aggregate structure (Source: Möhwald, et al. 1993)

Dye aggregates have many applications such as in optoelectronics (Moliton, et al. 2004) , sensor devices (Jones, et al. 2001), fast optical recording systems (Naber, et al. 1999), high resolution optical recording systems (Kodaira, et al. 2007) and light harvesting systems (Kirstein, et al. 2006).

The most well-known example of the cyanine dyes is Pseudoisocyanine (PIC) dye, which is a simple cyanine molecule. Molecular structure of PIC-Br is given in Figure 1.8a. Spectroscopic studies on PIC aggregates date back to the midthirties when Jelley and Scheibe independently discovered that concentrated solutions of PIC-Cl develop a sharp absorption band. It can form J-type of aggregates at concentrations of micromolars. TTBC (Figure 1.8b) is also another cyanine dye which is a carbocyanine. Different than PIC, it can form two types aggregates, J- and H-types. It can be aggregated at concentrations of nanomolar levels.

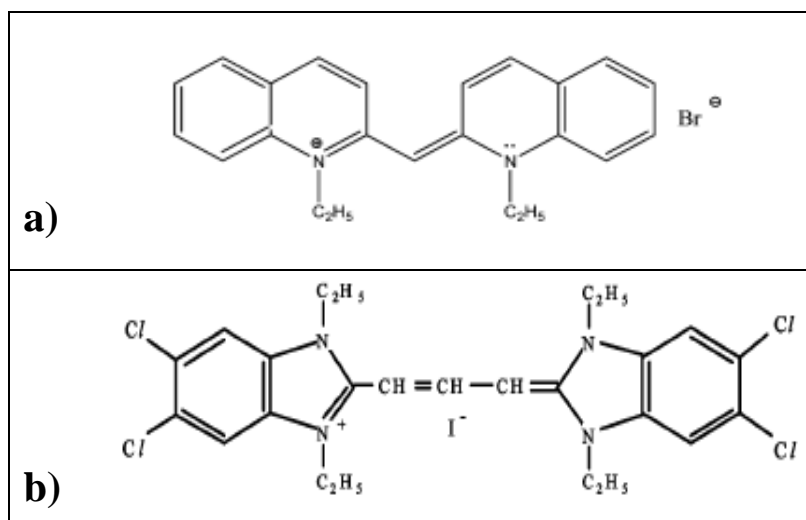


Figure 1.8. Molecular structure of a) Pseudoisocyanine-Bromide (PIC-Br), b) 1,1',3,3'-tetraethyl-5,5',6,6'-tetrachlorobenzimidazolocarbocyanine-Iodide (TTBC)

1.3. Combination of Self-assembly and Electrospinning

The combination of self-assembly and electrospinning approaches integrates advantages of both techniques. There are few reported studies that combine these two phenomena. Kuo et al. studied electrospinning of [2,7-(9,9-dihexylfluorene)]-block-poly(methyl methacrylate) (PF-b-PMMA) which are rod-coil block copolymers (Kuo, et al. 2008). They found that different aggregated structures of PF block (dot-like, line-like and ellipse-like) within nanofibers can be obtained by only changing DMF/THF solvent ratios

of precursor solution in electrospinning. As a result, these electrospun fibers with different aggregate morphologies leads to different photophysical properties through use of selective solvent. Furthermore, fabrication of PDA-embedded PEO fibers studied by Chae et al. They electrospun PEO solution with individually dispersed DA monomers (Chae, et al. 2007). To investigate the self-assembly of DA monomers within the fibers, the fiber mat was irradiated with UV light. Upon irradiation, the fiber developed a blue color, suggesting that PDAs were produced from supramolecularly assembled crystalline or semi-crystalline diacetylene monomers. This observation confirms that the well ordered DA monomers are created in the electrospinning process. Otherwise polymerization could not be take place. In addition, Kalra et al. showed microphase separation as cylindrical and lamellar morphology in electrospun PS-b-PI nanofibers (Kalra, et al. 2006). They reported that by the block copolymer composition, the length, shape and distribution of these worm-like entities can be controlled in a systematic form. Moreover, Kim et al. studied the arrangement of gold nanoparticles within the fibers by electrospinning with PEO and shows that electrospinning is an straightforward and cost effective technique to produce one-dimensional nanoparticle arrays for future nanodevices (Kim, et al. 2005). Furthermore, electrospinning of polycarbonate urethane (PCU) with CdSe nanoparticles studied by Demir, et al. 2009 . They reported that electrospinning provides self organization of PCU domains and modifies the emission of CdSe nanoparticles. All these literature works reported here, show that electrospinning (top-down approach) and self assembly (the bottom-up approach) can be succesfully combined and form fine hierarchical nanostructures.

In our previous work (Demir, et al. 2009), we have combined the formation of J-aggregate and electrospinning processes using PIC and PVA system in aqueous alcoholic solutions. PIC is one of the frequently used cyanine dye which form only one-dimensional fibrous-like J-aggregate. Although PIC molecules were individually dispersed in precursor solution, they assemble into J-aggregates upon electrospinning process. The results also showed that electrospinning not only provided the formation of J-aggregate but also allows orientation of J-aggregates along the fiber axis. Consequently, electrospinning was found to be an efficient approach to form molecular aggregates of cyanine dyes. In this study, using the same polymer/solution system, we employed another cyanine dye, TTBC, which has, not one but two types of aggregates (H and J-type). The main theme of this work is to control the type of aggregation by instrumental and solution parameters of electrospinning process.

CHAPTER 2

EXPERIMENTAL STUDY

2.1. Materials

All dye and polymers were used as received from the manufacturer without further purification. For solution preparation distilled water, methanol and dimethylformamide (DMF) were used as solvent. PVA with 87-90% hydrolyzed and 30-70 kg · mol⁻¹ molecular weight was obtained from Sigma-Aldrich, USA. Water and DMF were used as solvents for PVA and PS, respectively. TTBC and TDBC were obtained from Hayashibara Biochemical, Co., Okayama, Japan, and used as-received. The methanol was used as solvent for TTBC solutions. Pyrene was provided by Alfa Aesar A. Johnson Matthey Ccompany and Sigma-Aldrich, USA, respectively.

2.2. Experimental

2.2.1. Preparation of Precursor Solutions

PVA and TTBC solution were prepared in distilled water and methanol respectively. 1mL of alcoholic TTBC solutions were dispersed in aqueous PVA with same volume fractions at room temperature. Concentrations and weight percents of TTBC/PVA solutions were given at Table 2.1.

Table 2.1. TTBC/ PVA contents in their solutions

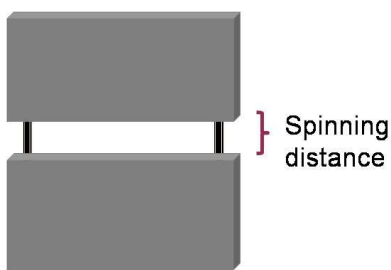
	[TTBC] in methanol (mM)	PVA in water (wt %)	TTBC/PVA (wt %)
1	0.025	10	0.001
2	0.05	10	0.033
3	0.1	10	0.163
4	0.5	10	0.326
5	1.0	10	0.652
6	0.5	7.5	0.435
7	0.5	12.5	0.240
8	0.5	15	0.218

Pyrene was dissolved in DMF and dispersed in Polystyrene/DMF solution. Dispersions prepared at six different pyrene concentrations (10^{-7} , 10^{-5} , 10^{-3} , 10^{-1} , 10 mM and 1M) while polystyrene content was kept constant at 25 wt%.

2.2.2. Preparation of Electrospun Films

The precursor solution of TTBC/PVA system that would be subjected to electrospinning process, was loaded to 1mL syringe. Microinfusion pump WZ-50C6 pushes the electrospinning solution out of the syringe needle at a flow rate of 0.5 ml/hr. Application of high voltage (6.7, 8.7, 12.7 kV) to the metal syringe needle allowed generation of nanofibers on the surface of the grounded collector. The collector was designed by two parallel stainless steel strips separated with 0.5 cm gap (Table 2.2b). Therefore, the electrospun fiber mat obtained on the collector was not homogeneous in nature. On the metal strips, e-spun fibers were randomly deposited. Moreover, aligned fibers were achieved between two strips. Hence, fiber populations consisting both isotropic and anisotropic were obtained by spinning of the same solution in a single run. The optimizations and instrumental parameter were given in Table 2.2a.

Table 2.2. a) Instrumental parameters and optimizations of electrospinning process, b) Electrode geometry

a		b
Applied potential difference (kV)	6.7 – 8.7 – 12.7	
Spinning distance (cm)	7	
Flow rate of precursor solutions (mL/hr)	0.5	

For Pyrene/PS electrospun fibers, instrumental optimizations were same as TTBC/PVA system but only the applied potential difference was 15kV.

2.2.3. Preparation of Spincoated Films

Spincoating set up illustrated in Figure 2.1. Spin coating is the preferred method for application of thin, uniform films to flat substrates. 1ml of sample solution is placed on the glass substrate. The substrate is then rotated at high speed in order to spread the fluid by centrifugal force. Rotation is continued for 1 minute, with fluid being spun off the edges of the substrate.

The spincoated films of TTBC/PVA solutions prepared by using WS 400B 6NPP/LITE at different TTBC concentrations ranging from 0.025 to 0.5 mM and rotation speed which are 1000, 2500 and 5000 rpm.

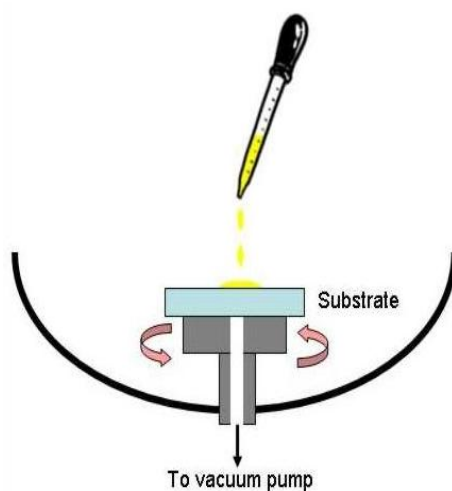


Figure 2.1. Schematic representation of spincoating process

2.2.4. Preparation of Cast Films

For each TTBC/PVA solutions, 500 μ L was dropped on to a flat glass surface. Glass surface washed with acetone and ethanol and dried to get rid of impurities and have a cleaned surface. They were left for evaporation of solvent in a dark environment. Film-casting set-up is shown in Figure 2.2.

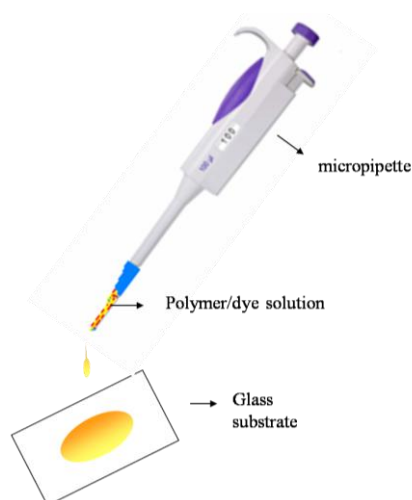


Figure 2.2. Schematic representation of cast film preparation

2.3. Characterization of Samples

2.3.1. Scanning Electron Microscopy

Phillips XL-30S FEG used to observe the morphology of nanofibers. Nanofibers with their substrate were coated with gold using magnetron sputter coating system (MSCS) for 60 seconds to reduce electron charging effects. The average fiber diameter analysis was performed using image analysis software (ImageJ, NIH, USA) from >50 randomly selected.

2.3.2. Polarized Fourier Transform Infrared Spectroscopy

Polarization and chemical characteristics of electrospun fibers were evaluated by recording infrared spectra using Perkin-Elmer Spectrum 100 Fourier Transform Infrared Spectrometer with a polarizer (ZnSe). By changing the polarization angle, the absorbance was recorded at 0 and 90° with respect to aligned fibers. Samples were scanned at operating wavelengths in the range between 4000 and 600 cm^{-1} . Each measurement was composed of an average of 4 scans at a resolution of 4 cm^{-1} .

2.3.3. Photoluminescence Spectroscopy

Varian Eclips spectrofluorometer was used for investigating the emission feature of samples. All samples (solutions, cast and spincoated films, random and alligned fibers) were analyzed for photoluminescence measurements. The working wavelength range was 480-700nm where the samples excited at 450nm.

For alligned and random fibers, polarized photoluminescence spectroscopy was used by the help of two polarizers. One of the polarizer placed in front of the incoming light, the other one was, to polarize the emmiting light, placed in front of the detector. Polarizers were placed horizontally and vertically, respectively. Therefore, for one sample, there are four different spectrum were taken at different polarizer combinations which are vertical-vertical, vertical-horizontal, horizontal-horizontal, horizontal-vertical. Schematic representation of measurement set up is shown in Figure 2.3.

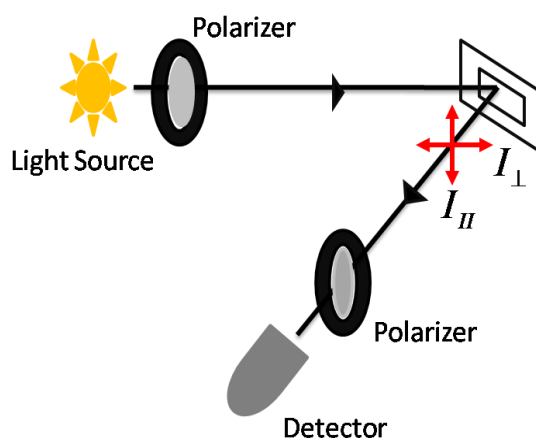


Figure 2.3. Schematic representation of polarized emission spectrometer

2.3.4. UV-Visible Spectroscopy

UV-Vis spectroscopy also used to analyze the structures of dye molecules in solutions. For UV-Vis absorption measurements, the working wavelength range was 300-700nm.

CHAPTER 3

RESULTS AND DISCUSSIONS

In this study, several polymer/pigment systems have been tried. They were TTBC/PVA in an aqueous solution, TTBC/PS and Py/PS in DMF solution. The majority of work was focused on TTBC. The results are given in detail consequently in the following.

3.1. Electrospinning of PVA Solution

At the beginning of the study, only PVA fibers were prepared from 10(wt)% aqueous PVA solution without any pigment. The fibers were examined in terms of alignment of fibers and orientation of PVA chains.

Electrospinning process, in general, provides randomly-deposited fibers. The arrangement of the fibers in fact depends on geometry of the electrodes. In a continuous metal sheet, electrical field lines start from solution droplet through the surface of collector (Figure 3.1a). The lines have preferential direction to the normal of the surface of collector sheet, as a result, randomly deposited fibers are obtained. However when two parallel positioned grounded collector with a void gap is used, electrical field lines are directed toward the edge of metal collectors (Figure 3.1b). The charged fibers has moved into the vicinity of the collector, charges on the fibers induce an opposite charges on the surface of it. When the fibers attract to the collector, electrostatic forces pull the fibers towards the edge of the collectors and the fibers deposited across the gap as uniaxially aligned arrays.

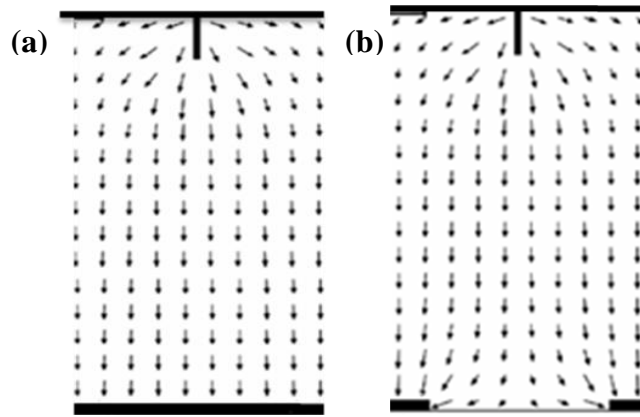


Figure 3.1. Electrical field lines between tip of the needle and collector in electrospinning process (a) a plate-like electrode that results in randomly deposited fibers, (b) a pair of parallel-positioned metal strips separated with an air gap to fabricate uniaxially aligned fiber between two strips (Source: Li, et al. 2003)

For the reason of achievement of aligned fibers, the collector was designed by two parallel metal strips separated by a void gap. An overview of the collector system was imaged by a scanning electron microscope (Figure 3.2a). The geometry of the electrode leads to two types of fiber deposition. On the metal strips, PVA fibers were randomly deposited, they had no preferential direction (Figure 3.2b). However, PVA fibers formed across the gap were appeared to be aligned perpendicular to the long edge of the strips (Figure 3.2c). Hence, electrospun film consisting of both isotropic and anisotropic fiber populations was obtained by spinning of the same solution in a single run.

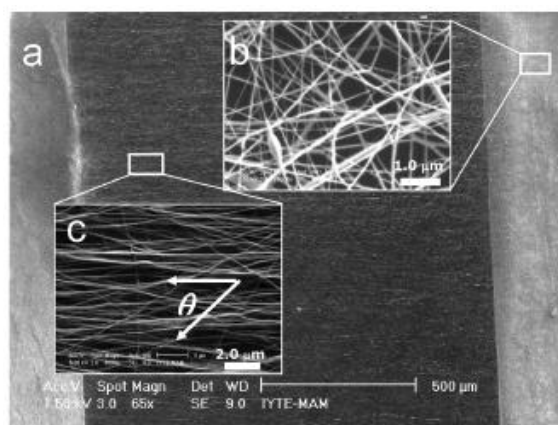


Figure 3.2. SEM micrograph of a) electrode and the e-spun fibers, b) randomly deposited PVA fibers collected on the surface of collector, c) uniaxially aligned fibers across the void gap

The degree of alignment of PVA fibers was achieved by measuring the angle between the fibers and normal of the metal strips for more than 100 fibers. The majority of fibers fall in the range of 0-10 degree (Figure 3.3) suggesting a high degree of alignment.

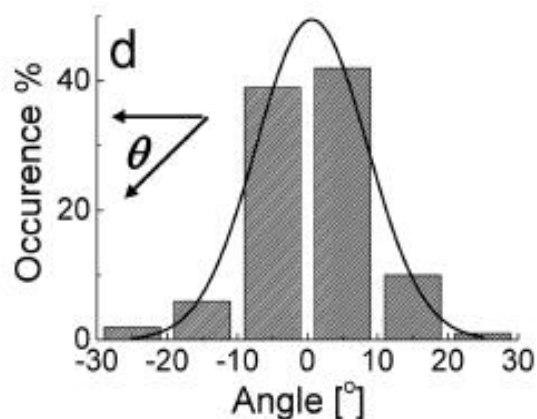


Figure 3.3. Histogram of the angle (θ) between the long axis of fibers and the normal of the long edge of the metal electrodes

SEM images showed the **macroscopic** alignment of e-spun fibers. For **microscopic** investigation, the morphology in terms of **molecular orientation** of PVA chains was performed by polarized FTIR spectroscopy where an IR beam probe was polarized parallel and perpendicular to the fiber axis. Figure 3.4a shows the polarized FTIR spectrum of randomly deposited and uniaxially aligned fibers of TTBC/PVA system. Parallel and perpendicularly polarized spectra of randomly deposited fibers are almost identical. This result indicates the isotropic feature of randomly oriented fibers. However, for aligned fibers, polarized FTIR spectra shows remarkable intensity differences depending on the polarization of the incident IR beam. This behavior can be correlated with the orientation of PVA backbone in the fiber direction. PVA molecules composed of carbon atoms on the backbone (Figure 3.4c) and C-C bond is parallel to the backbone of the chain. On the other hand, pendant oxygen of hydroxyl or acetate groups (C-O) is perpendicular to the backbone. Therefore, the comparison of absorbance of the backbone and pendant vibrations in parallel and perpendicularly polarized FTIR spectrum provides a valuable insight to understanding of internal orientation of PVA chains within PVA fibers. When the incident IR beam is parallel polarized to the fiber axis, it interacts with higher number of C-C bonds with respect to perpendicular polarized one and result in higher intensity of backbone vibration at 2942 cm^{-1} . However, when the beam is perpendicularly polarized, the interaction of light with

C-O bond is more and have higher intensity at 1097 cm^{-1} in the spectra. Based on these results, it can be proposed that PVA chains are oriented along the fiber axis. The orientation of polymer chains can be related with the large dipole moment of water molecules and PVA chains. By the induced electrical field during electrospinning process, water dipoles tend to orient and in turn align the polymer backbone in the fiber direction.

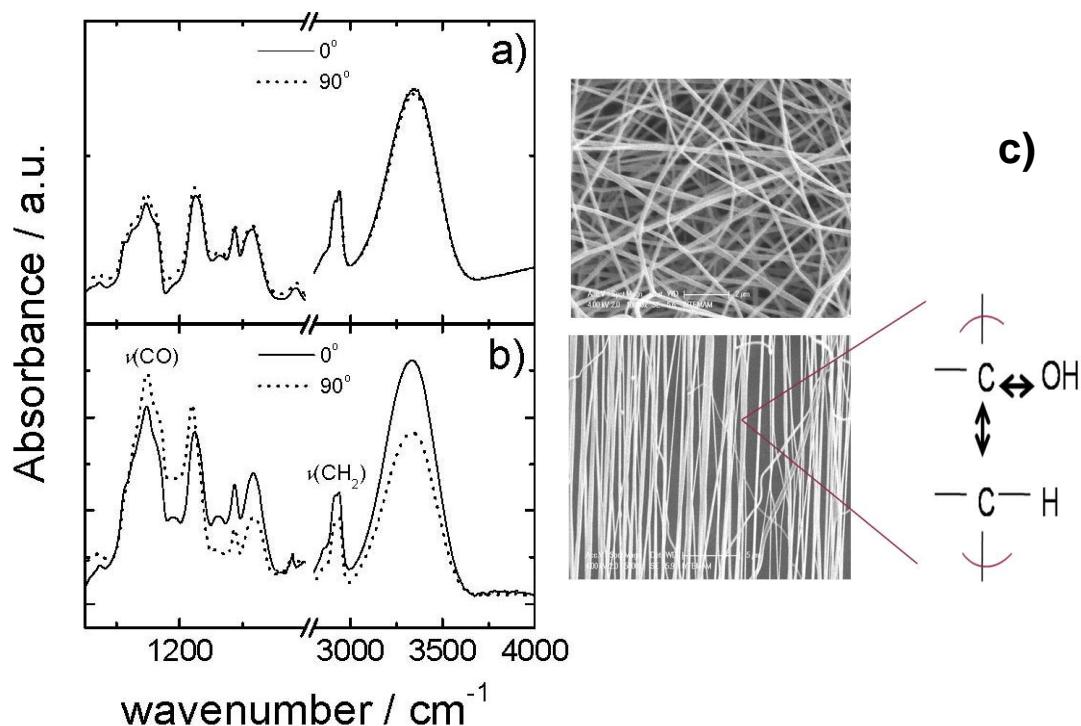


Figure 3.4. Polarized FTIR spectra of a) randomly deposited, b) aligned PVA fibers that electrospun at 1.6 kV/cm , c) macroscopic alignment of e-spun fibers and monomeric residue of PVA.

PVA solutions were subjected to electrospinning process with fluorescent molecules as an additive. For this reason, it should be proven that the emission was coming from these molecules only, not from PVA. Therefore, only PVA fibers that were prepared without any pigment were examined by photoluminescence spectroscopy. The emission spectra of PVA fibers were obtained where the excitation wavelength was 450 nm . The reason of choosing 450 nm is that it is the excitation wavelength of TTBC dye which resulted in highest intensity. Figure 3.5 shows the PL spectra of PVA fibers. There is no signal observed so this indicates that there is no emission of PVA molecules.

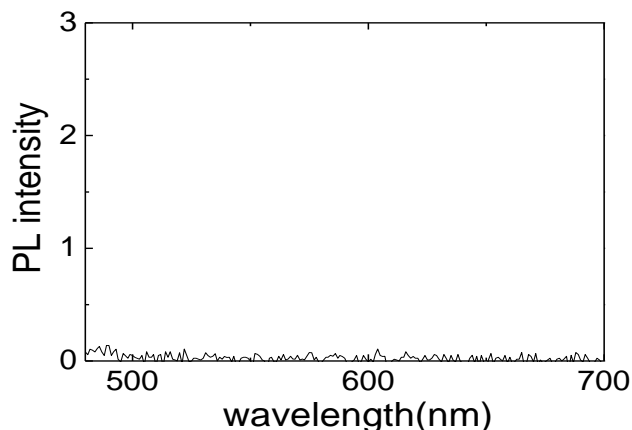


Figure 3.5. PL spectra of electrospun PVA fibers

3.2. Electrospinnig of TTBC Monomer/ PVA Solution

The main idea of this study is to examine the effect of electrospinning on molecular aggregation of TTBC. Therefore, the electrospinning solution should have no aggregate. In this sense, TTBC/PVA precursor solutions were examined by UV spectroscopy initially. The spectra of various concentrations ranging from 0.025 to 0.5 mM exhibits the absorption band of TTBC monomers in PVA at 520 nm (Figure 3.6). This result proves that TTBC molecules were individually dispersed in solution, and the spinning solution was initially free of aggregates.

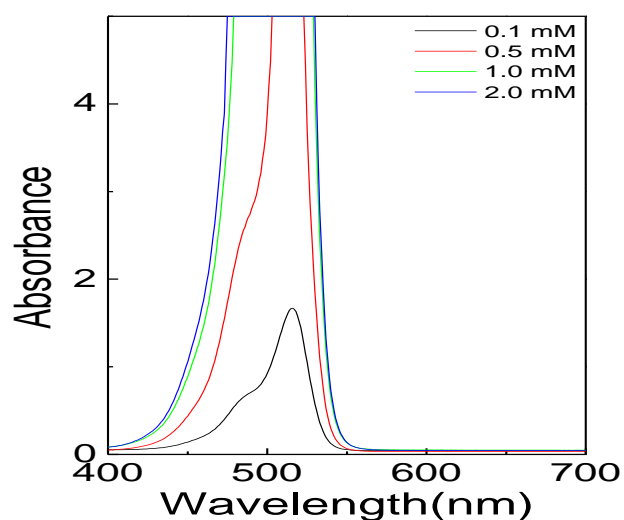
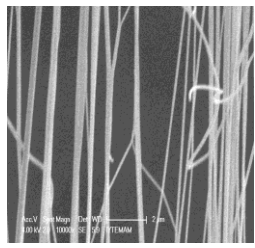
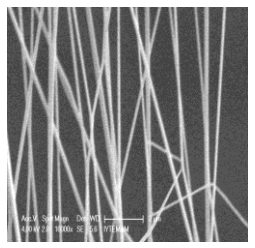
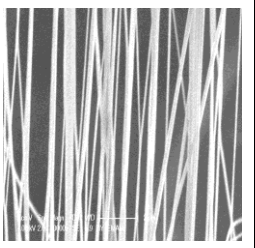
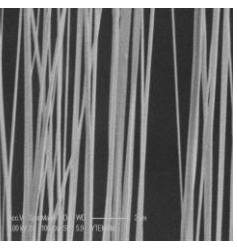
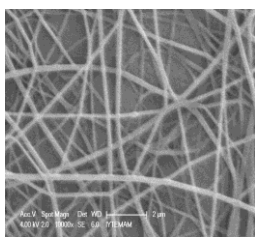
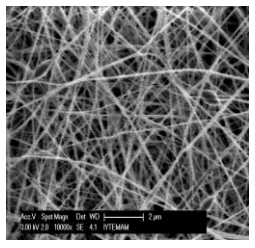
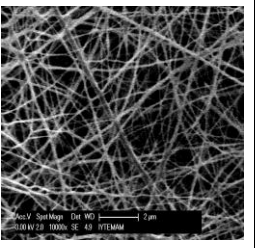
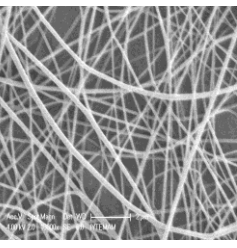


Figure 3.6. Absorption spectra of TTBC methanol solution at different concentrations

3.2.1. The Effect of [TTBC] on Molecular Aggregation

The monomeric TTBC/PVA solutions were subjected to electrospinning process at different [TTBC] ranging from 0.025 to 0.5 mM. The applied potential difference was kept constant at 12.7kV. Table 3.1 represents the SEM images of resultant TTBC/PVA electrospun fibers.

Table 3.1. SEM micrograph of a) aligned and b) randomly deposited fibers electrospun from %10 PVA solution at different [TTBC] (magnifications at 10,000 \times)

	0.05 mM	0.25 mM	0.5 mM	1.0 mM
Aligned fibers				
Random fibers				

The average fiber diameters (AFD) of TTBC/PVA fibers were measured to investigate the effect of TTBC concentration on PVA fiber diameters. The results (Figure 3.7) showed that as TTBC concentration increases in precursor solution, the diameter of fibers slightly increases. This could be the result of chemical nature of TTBC. It is a salt molecule so it increases the charge density in precursor solution and enhances elongational strain that should makes the fibers thinner. On the other hand, the salt increases the electric current and accordingly mass transfer. Increasing mass transfer enlarges the diameter of fibers. In these particular experiments, these two counter effects balance each other and it can be concluded that AFD was found to be independent of TTBC concentration.

Moreover, it is observed that aligned fibers were thinner than random fibers. The aligned fibers deposited across the gap so there was no substrate behind them. This leads to an additional stretching of fibers and makes the fibers thinner.

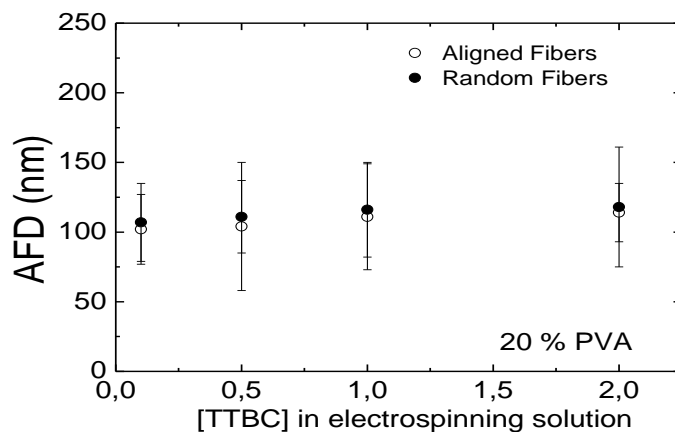


Figure 3.7. Average fiber diameters at different [TTBC]

Structural analysis of dye molecules within electrospun fibers were performed by photoluminescence (PL) spectroscopy. The spectra were normalized with respect to monomers to follow the extend of aggregation. Figure 3.8a and b show the normalized emission spectrum of randomly-deposited and aligned PVA/TTBC fibers electrospun at different TTBC concentrations. There are two bands observed at 485 and 535 nm corresponding to H-band and monomer band, respectively. Therefore, there were only H-aggregate and small amount of monomers remained within both random and aligned fibers. No J-aggregate formation was obtained. Moreover, the emission of H-band generally could not be observed in solutions or interfaces but in our particular case, the H-aggregates were formed in a concentrated polymeric media and confined to one-dimensional of fibers. Furthermore, increase in TTBC concentration resulted in a decrease of H-band intensity with respect to monomer. At higher TTBC concentration, the applied electrical force during process is not enough to create more H-aggregates could be the result of this behavior. In addition, comparison of emission spectrum of random and aligned fibers indicate that aligned fibers have higher H-band intensity than random fibers with respect to monomer intensity. This can be correlated with the higher electrical field that aligned fibers exposed to during process.

The formation of only H-type rather than J-type aggregates can be the result of the molecular structure of TTBC because the heterocyclic rings are positioned at angle 4° with respect to each other. In other words, it is almost a planar molecule. Therefore,

it can be aggregated easily. Moreover, in electrospinning process, very high electrical force is applied in the kV range. For this reason, rather than J-aggregates, TTBC molecules can be arranged almost parallel and form H-aggregates.

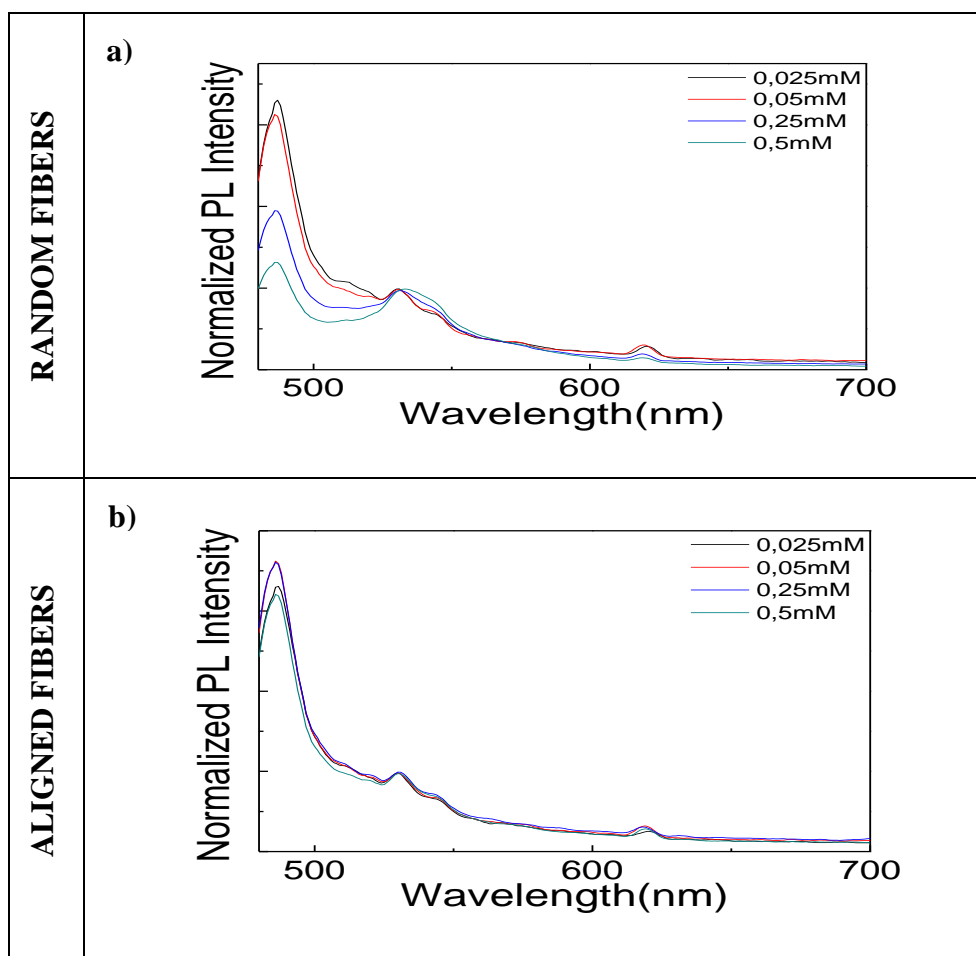


Figure 3.8. a) PL spectrum of TTBC/PVA randomly deposited fibers, b) Aligned fibers prepared at different [TTBC] (excitation wavelength: 450nm)

3.2.2. The Effect of Potential Difference on Molecular Aggregation

As an important instrumental parameter, the electrospinning was performed at different potential differences which were 6.7, 8.7 and 12.7 kV. The emission spectrum of resultant fibers are shown in Figure 3.9. There are H-aggregates and monomers within fibers and J aggregate formation was not observed. Increment of potential difference enhances the formation of H-aggregates. This is because, in electrospinning process, the applied potential difference create an electrical force on the surface of the droplet and also an electrical field between the tip of needle and collector. As the applied potential difference increase, the strength of electrical field accordingly the

force acting on TTBC molecules increase. Finally this augmentation forced TTBC monomers to come together and form high amount of H-aggregates.

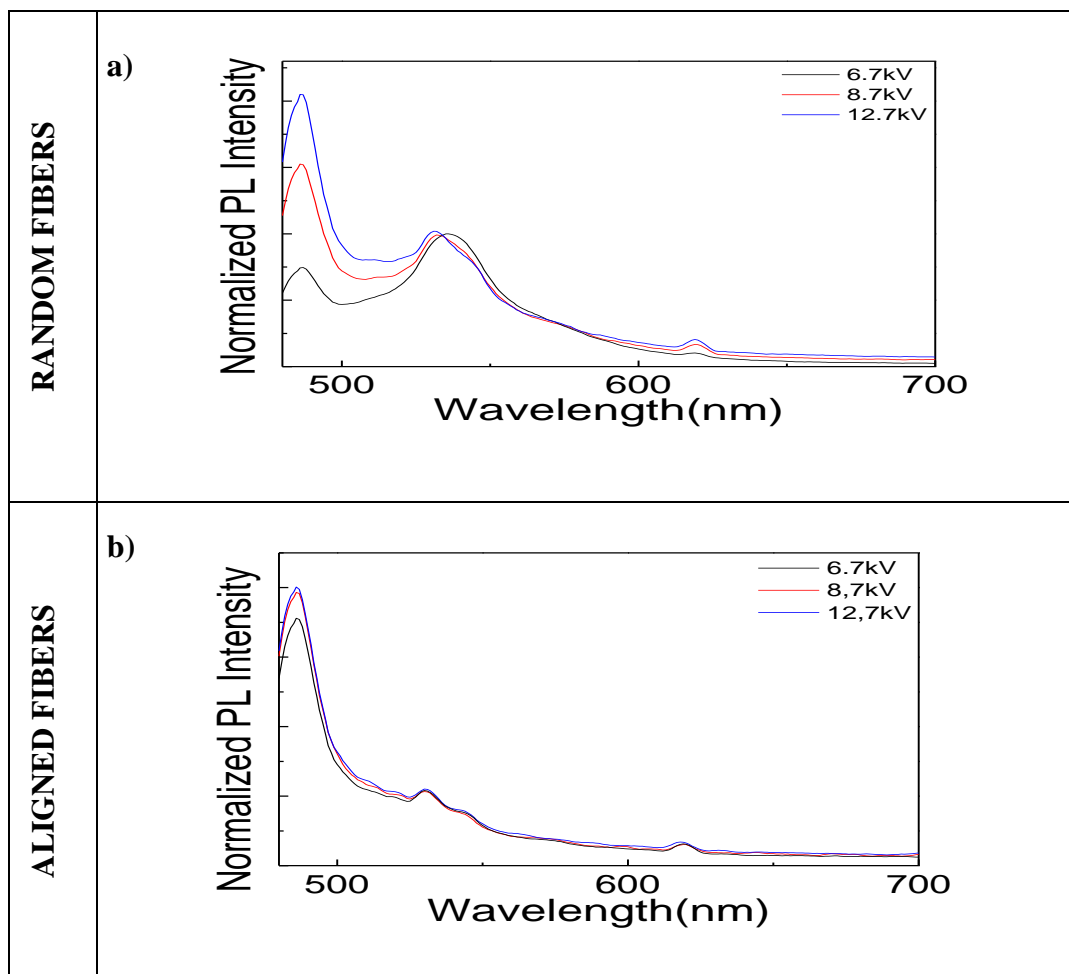


Figure 3.9. PL spectrum of a) randomly-deposited, b) Aligned fibers e-spun from 0.5 mM TTBC/PVA 10% at different potential differences

Polarized FTIR spectroscopy was used to analyze the effect of applied potential difference and TTBC concentration on orientation of PVA chains. To do this, the polarized FTIR spectrum of the fibers electrospun at different potential difference and TTBC concentrations were registered. An additional set of data were obtained by the help of examination on FTIR data of each sample. The calculations were done using the absorbance values of the vibration bands of CO and CH₂ stretching of PVA. For each spectra, the dichroic ratios of PVA chains at 1097cm⁻¹ (CO) and 2942 cm⁻¹ (CH₂) were calculated. The two dichroic ratio of each sample were proportionated to each other. Therefore, the polarization at 2942cm⁻¹ was normalized to 1097 cm⁻¹. These calculations were performed to quantify the polarization more precise because

normalization was done according to the bands in the same spectrum. The resultant values showing the effect of TTBC concentration and potential difference on alignment of fibers were shown as a graph in Figure 3.10. According to these results, increasing TTBC concentration result in increment of chain orientation within fibers. This result can be correlated with the ionic character of TTBC. Increment of ion concentration induce electric field at constant potential difference. As a result, more electric field acts on polymer chains, orientation of the chains is induced in the fiber direction.

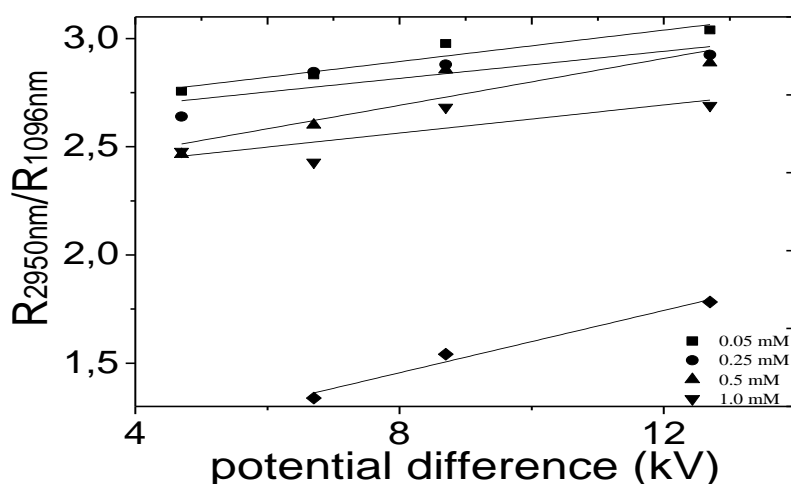


Figure 3.10. FTIR polarization graph of TTBC within PVA fibers

Investigations on orientation of H-aggregates within the fibers of TTBC/PVA system were performed by polarized PL Spectroscopy. Figure 3.11a and b respectively show the polarized spectrum of aligned and randomly deposited electrospun fibers obtained from TTBC/PVA solution. For aligned fibers very strong polarized emission was observed when light was parallel polarized and for other three polarizations, the intensity decreased remarkably. The degree of orientation of H-aggregates quantified by the dichroic ratio. For aligned and random fibers, dichroic ratios of H-band are 29 and 5, respectively. This polarization dependence indicates that the orientation of H-aggregates on the direction of PVA fibers. Even if less than aligned one, randomly deposited fibers also showed polarization dependence. It may be related to formation of aggregates not only parallel but also perpendicular to the axis of fibers.

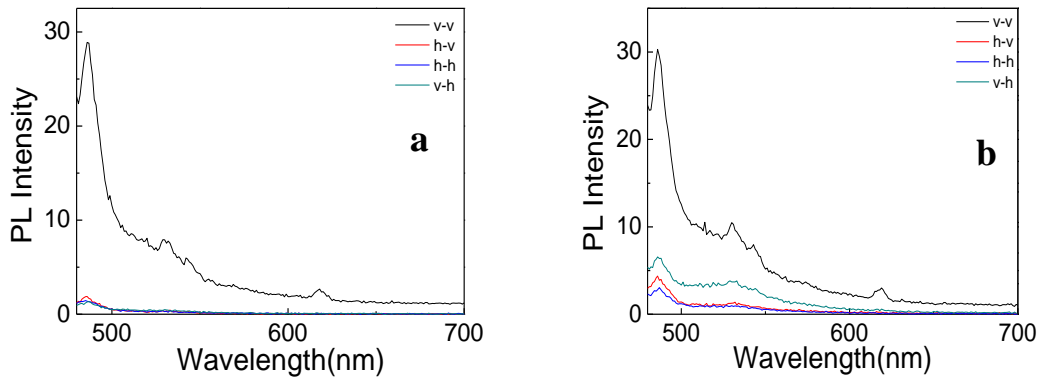


Figure 3.11. Polarized PL spectrum of a) aligned and b) random fibers of TTBC/PVA system performed at four different polarizer combination which are vertical-vertical, vertical-horizontal, horizontal-horizontal and horizontal-vertical with respect to the aligned fibers of 0.5 mM TTBC/PVA(10 wt%) prepared at 12.7kV.

Based on polarized PL spectroscopy results, an organization of H-aggregates within fibers can be proposed. Figure 3.12 shows the cartoon demonstration of this structure. Each lines represent the transition dipole moments of TTBC molecules. The angle between molecular axes and the transition dipole moments must be larger than 54° due to formation of H-aggregates. The transition dipole moments (d_2) are equidistant and parallel to each other. However, it is so small with respect to interchain separation (d_3) Also, the distance between two aggregates is much higher than d_2 and d_3 The dipole moment of the each aggregate was represented by $\mu_{aggregate}$. Therefore H-aggregates formed in the fibers and they are parallel to the fiber direction.

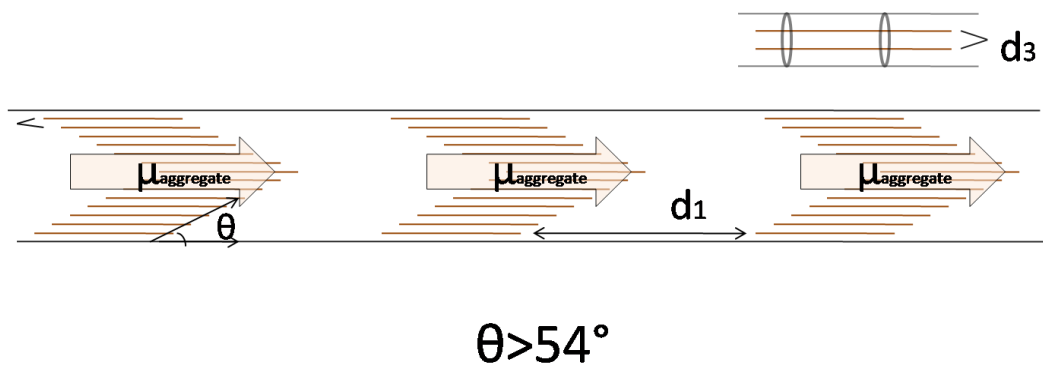


Figure 3.12. Cartoon demonstration of aggregates within fibers (A crosssectional view)

The alignment of fibers with aggregates were also confirmed by polarized optical microscopy. Figure 3.13 represents the polarized microscope images of aligned

fibers of TTBC/PVA which were performed at different polarization angles. The images belong to one sample, only the polarization angle is different. Changing polarization angle of light was allowed to observe only aligned or randomly deposited fiber layers, separately. The aligned fiber layer was obtained light polarized at 20° and the sample and the other polarizer under the sample was stable.

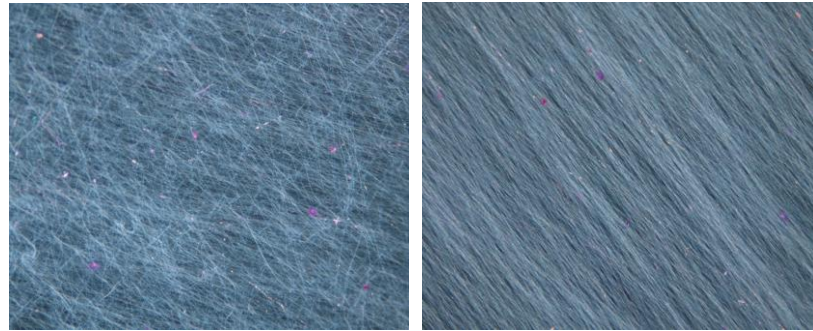


Figure 3.13. Polarized microscope images of aligned fibers performed at different polarization angles (the fibers prepared from 0.5 mM TTBC/PVA solution at 12.7 kV)

3.2.3. The Effect of Fiber Diameter on Molecular Aggregation

The dominant solution parameter in electrospinning process is the polymer concentration. The precursor TTBC/PVA solutions were electrospun at different PVA contents. TTBC concentration was kept constant at 0.5 mM while PVA content was varied from 7.5 to 15 (wt)%. SEM images of the resultant fibers are given in Table 3.2.

Table 3.2. SEM micrographs of aligned and random PVA/TTBC electrospun fibers at constant [TTBC] but different PVA content

	7.5 wt%	10.0 wt%	12.5 wt%	15.0 wt%
Aligned fibers				
Random fibers				

The average fiber diameter of these fibers are given in Figure 3.14. It shows that the diameter of fiber increases as PVA concentration increases. This result is not surprising because as the polymer concentration increases, the entanglement of polymer chains increases also the viscoelastic force increases. Hence, the charged jet is prevented to break-up into smaller jets. As a result, the fibers that are produced from high polymer concentrations have larger fiber diameters.

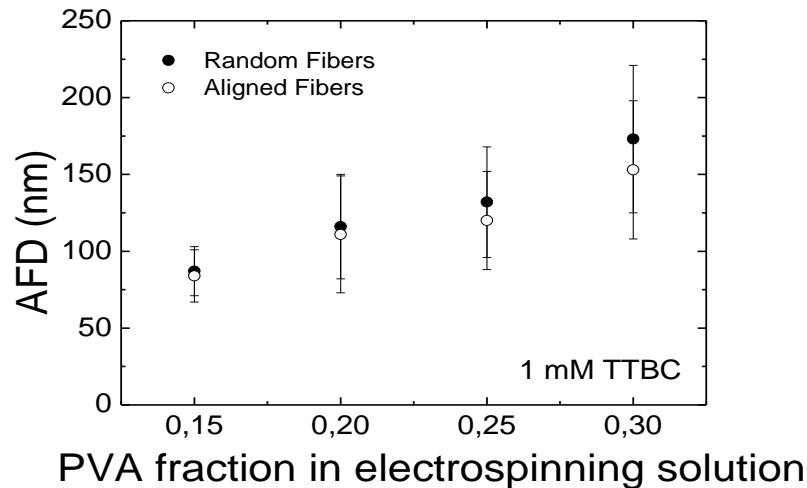


Figure 3.14. Average fiber diameters versus PVA fraction

The aim of varying PVA content was to investigate the effect of fiber diameter on TTBC aggregate formation. However, as it is shown in Figure 3.15, the PL spectra of different diameter fibers remain almost same. As a result, fiber diameter found to have no effect on aggregation process, at least in this range of concentration we employed.

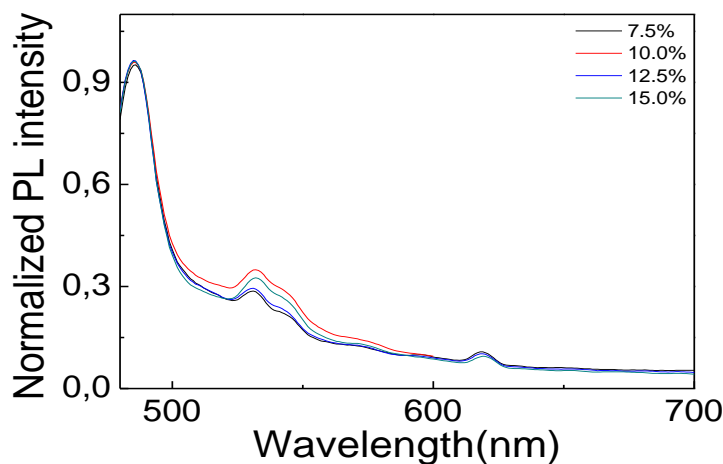


Figure 3.15. PL spectrum of electrospun fibers prepared at different PVA content (7.5- 10.0- 12.5- 15.0 wt %)

3.3. Electrospinning of J-aggregated TTBC

TTBC monomers in solution could be converted into H-aggregates within fibers by electrospinning. The question that need to be arised is that whether already aggregated solutions form fibrillar structures when they are subjected to electrospinning in absence of polymer.

3.3.1. In the Absence of Polymer

The most important criterion in fiber formation by electrospinning is the entanglement of long polymer chains consisting of covalently bonded monomer units and also the viscosity of the solution. Because of this feature, only polymers or polymer-like molecules result in formation of fibers. On the other hand, dye aggregates also have long molecular chains but bonded non-covalently and this property may cause formation of fibers or fiber-like structures with no need to polymers upon electrospinning. In this sense, an aggregated solution was prepared by addition of NaCl. NaCl causes J-aggregate formation in the solution because NaCl is a salt and it increases the ionic strength in solution. Therefore, TTBC molcules assemble and form aggregate to decrease the ion effect. The amount of NaCl is also important because as ion concentration increase in solution an energy transfer from J- to H-aggregates occurs and H-aggregates start to form (Birkan, et al. 2006). For that reason 0.01M which is low concentration of NaCl was used in 1mM aqueous TTBC solution. The PL spectra of J-aggregated solution is given in Figure 3.16.

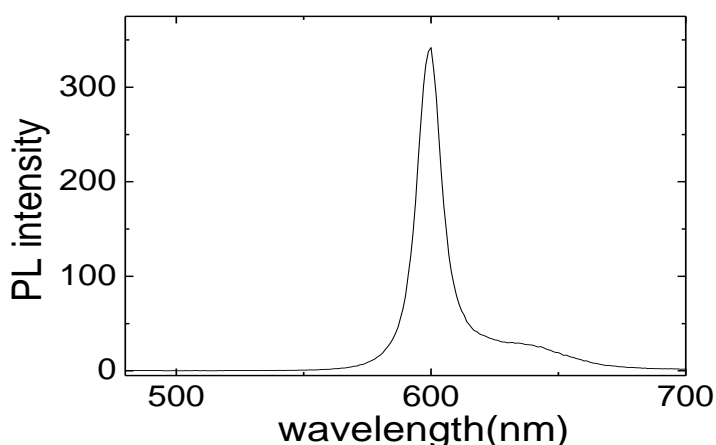


Figure 3.16. The PL spectra of J-aggregated TTBC solution

The solution was subjected to electrospinning process **without polymer**. SEM results indicated that electrospun samples of TTBC aggregates (Figure 3.17) were fiber-like structures even if they did not contain any polymer.

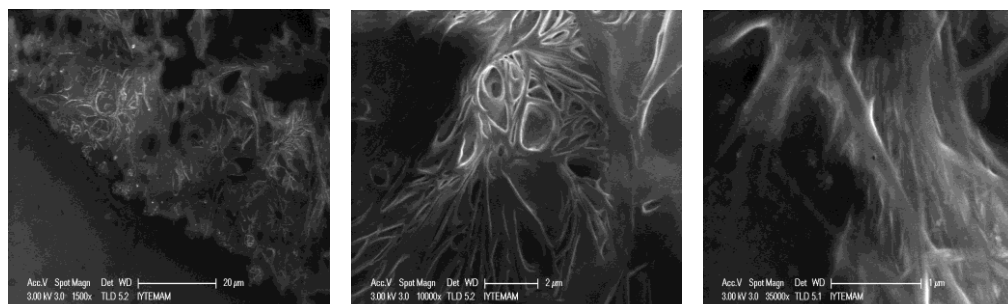


Figure 3.17. SEM images of resultant sample which were electrospun from J-aggregated solution of TTBC at 1500, 10000, 35000× magnifications, respectively.

The spectroscopic analysis of these structures is given in Figure 3.18 showing the formation of only H-aggregates. This is very similar result obtained from electrospinning of J-aggregated solution with polymer. Consequently, by the help of these two experiments, it can be concluded that the electrospinning process is able to convert not only monomers but also J-aggregates into H-aggregates within the fibers.

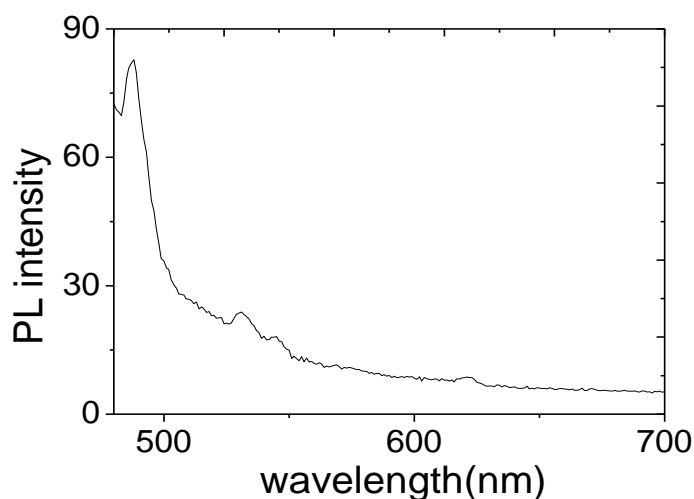


Figure 3.18. The PL spectra of electrospun TTBC sample

In addition to TTBC, 1,1'-diethyl-3,3'-di(4-sulfobutyl)- 5, 5', 6, 6'- tetrachloro benzimidazolocarbo-cyanine (TDBC) was used as another cyanine dye to investigate the aggregation process during electrospinning without polymer. TDBC shows very similar

properties with TTBC. It also undergoes both H- and J- type aggregates. Molecular structure of TDBC is given in Figure 3.19a. TDBC solution was prepared same as TTBC J-aggregated solution(1mM TDBC in 0.01M NaOH solution). The PL spectra of TDBC J-aggregates given in Figure 3.19b. Then the solution subjected to electrospinning.

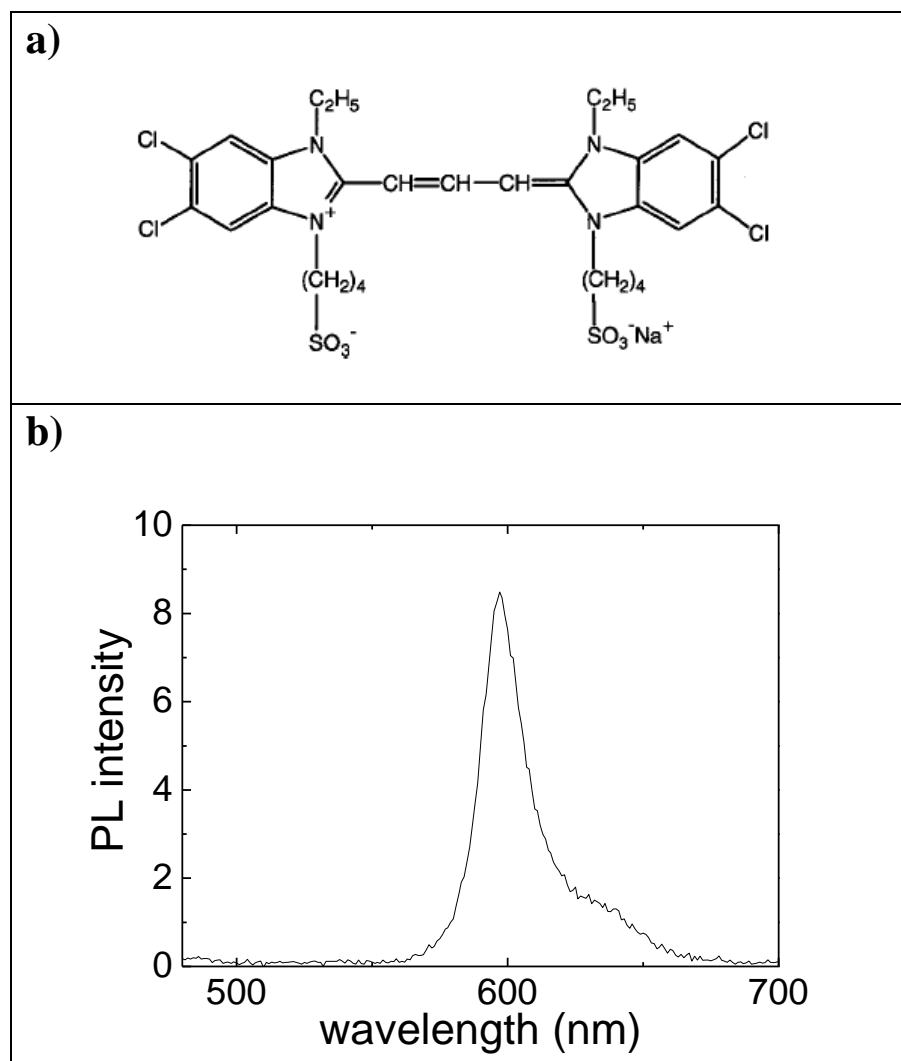


Figure 3.19. a) Molecular structure of TDBC b) The PL spectra of TDBC J-aggregates

SEM images of the resultant samples are shown in Figure 3.20 and they are fiber-like crystals. According to PL result (Figure 3.21), H-aggregates of TDBC molecules were obtained although they were J-aggregated in solution. It can be concluded as electrospinning has similar effect on aggregation properties of TDBC. Electrospinning induces the formation of molecular aggregates.

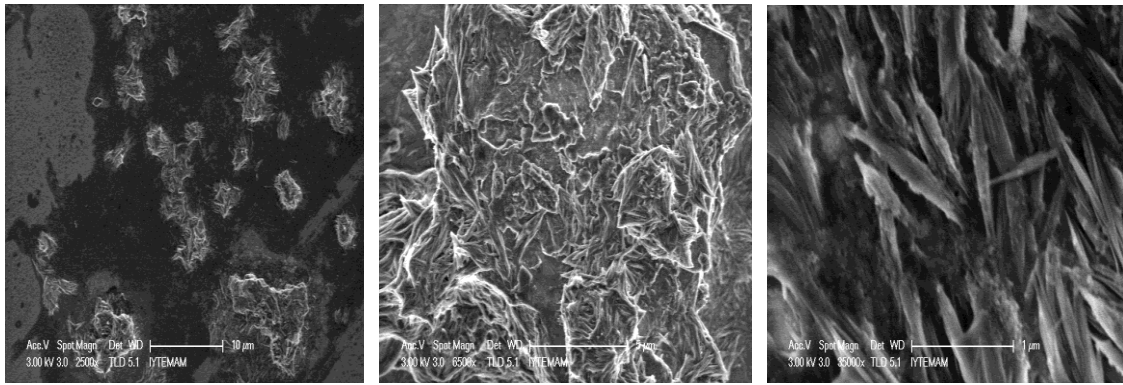


Figure 3.20. SEM images of electrospun TDBC sample at different magnifications (2500, 6500, 35000 \times , respectively)

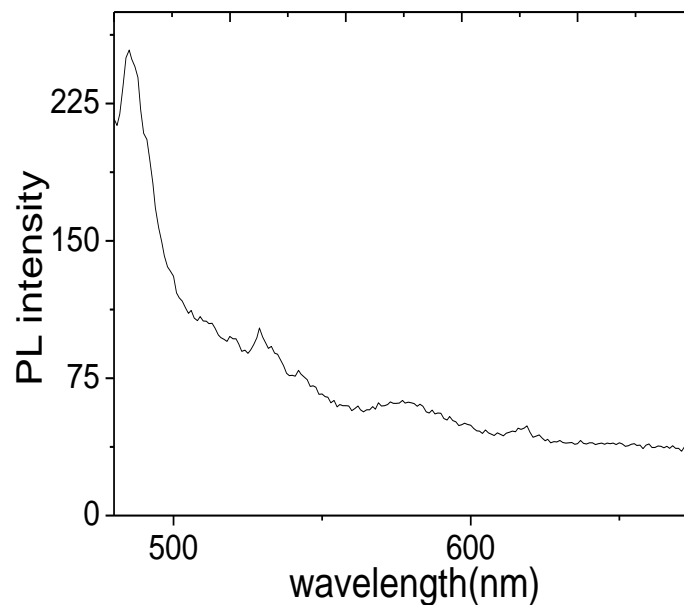


Figure 3.21. PL spectra of electrospun TDBC samples

3.3.2. In the Presence of Polymer

Aggregated solutions were also subjected to electrospinning in the presence of polymer. The spectra of J-aggregated TTBC/ PVA solution is given in Figure 3.22a. The sharp band observed at 590nm corresponds to the J-aggregates in the solution. The solution was then subjected to electrospinning process with PVA(10 wt%) at 12.7kV. The PL spectra of resultant fibers showed that H-aggregate formed within fibers where J-aggregates completely disappeared (Figure 3.22b).

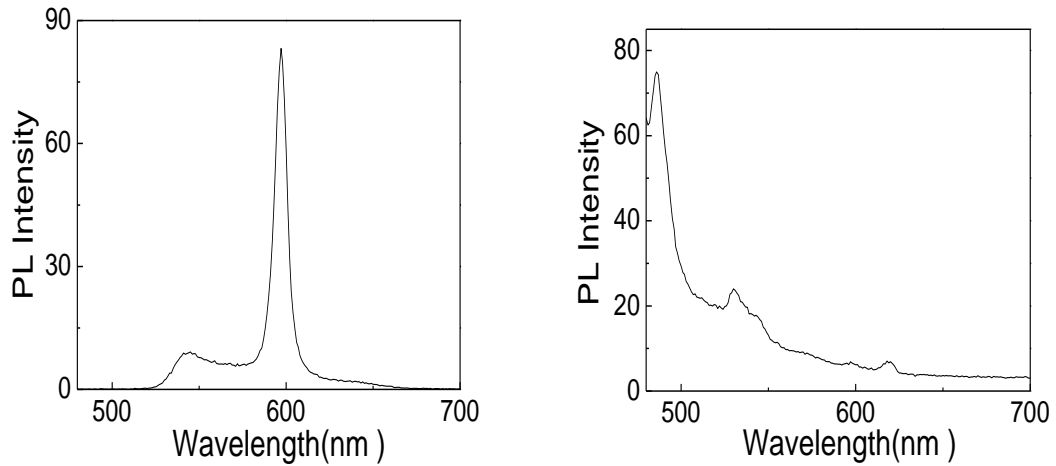


Figure 3.22. The emission spectra of a) J-aggregated TTBC in PVA solution, b) TTBC/PVA fibers electrospun from J-aggregated solution.

3.4. Comparison of Electrospun Mats with Spincoated and Cast Films

Two alternative thin film preparation techniques were used for the reason of comparison which were spincoating and film casting. Thin films of spincoating produced by centrifugal force. For film casting, there is no force applied, it is performed only dropping the solution on a solid surface. However, in electrospinning process, high electrical force is applied during the process. In addition to this, the sample produced by electrospinning is a thin fibrous film. As a result, comparison of three techniques helps the investigation of the effect of electrical force applied during process.

The photographic demonstrations of those films are given in Figure 3.23. While electrospun film is a fibrillour, spincoated film is continuous and its thickness is on the order of $2\mu\text{m}$. On the other hand, the cast film has a heterogenous surface and about $100\mu\text{m}$ thickness.

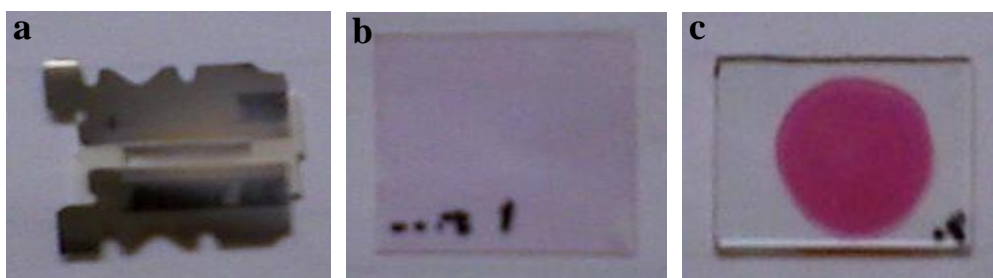


Figure 3.23. The photograph of a) electrospun, b) spincoated and c) cast film samples of TTBC/PVA solution

For spincoated films, different rotation speed ranging from 1000 rpm to 8000 rpm were applied. PL spectrum of these film samples are shown in Figure 3.24a. Spincoated films result both H and J-aggregates and as well as remarkable amount of monomers. Furthermore applying higher centrifugal force enhances the formation of both J and H-aggregates with respect to monomers. For cast film, there is only J aggregates of TTBC observed beside monomers (Figure 3.24b). Compared to spincoated film the formation of J-aggregates was favored within the film.

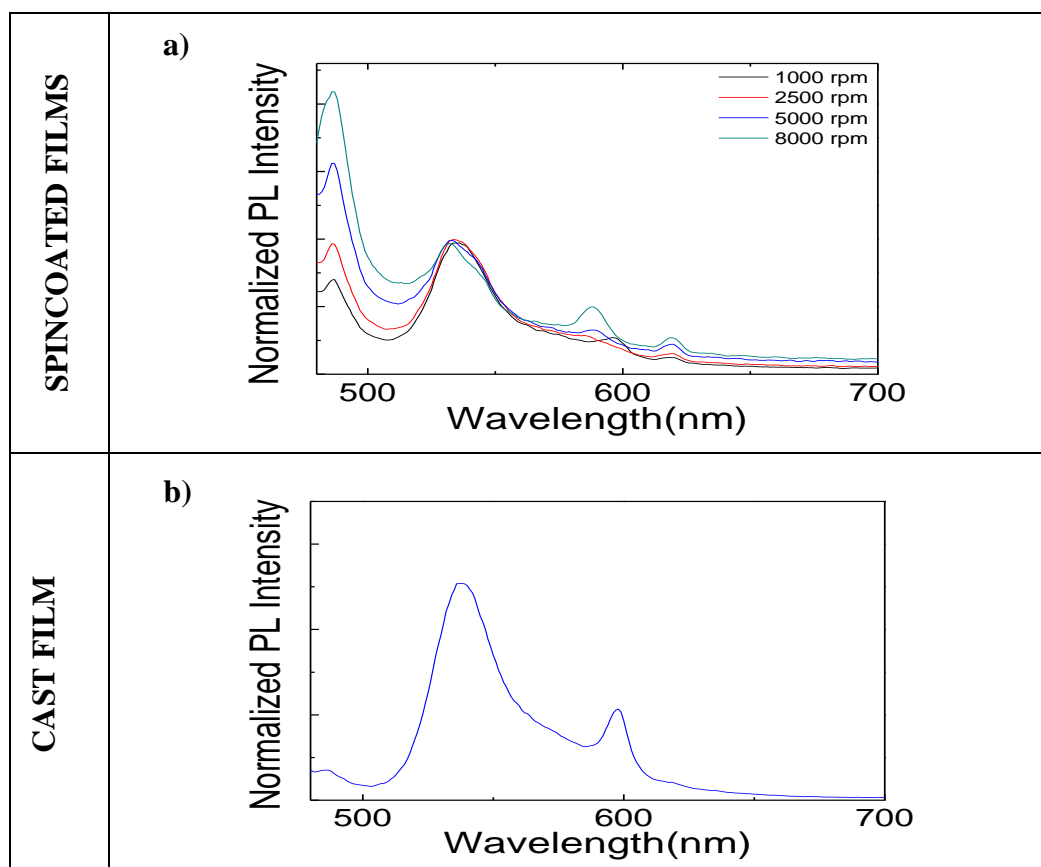


Figure 3.24. PL spectrum of A) Spincoated films prepared at different rotation speed, B) Cast film of TTBC(0.5 mM) /PVA (10 wt%)

The emission spectra of all TTBC/PVA thin film samples are given in one spectra (Figure 3.25) for the reason of comparison. Cast film of TTBC/PVA contains only monomer and H-aggregate where as spincoated film contains monomer, H and J-aggregate. However electrospun films, both randomly deposited and aligned fibers contain H-aggregate dominantly and there is a few amount of monomers. Comparison of three techniques resulted that as applied force during the process increase, the formation of H-aggregates dominate and J-aggregates disappear. Electrospun films

have more H-aggregates than other thin films because they exposed to higher electrical force in the range of kV.

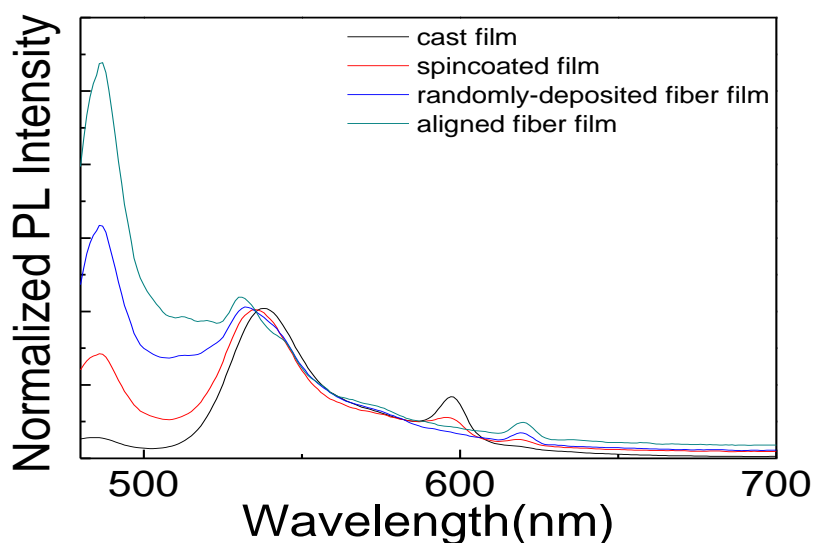


Figure 3.25. PL spectrum of TTBC/PVA thin film samples prepared by different film preparation techniques: Film casting, spincoating and electrospinning

3.5. TTBC Doped PS Fibers

In TTBC/polymer system, aqueous PVA solution was replaced with an organophilic PS in DMF. The question is whether similar type of aggregation occurs in an organic medium. Firstly, emission spectrum of precursor solution, TTBC/PS in DMF, was examined (Figure 3.26) and it is proved that the solution composes of TTBC monomers, only. There is a red-shift of monomer band about 10 nm caused by high concentration (1mM) of TTBC.

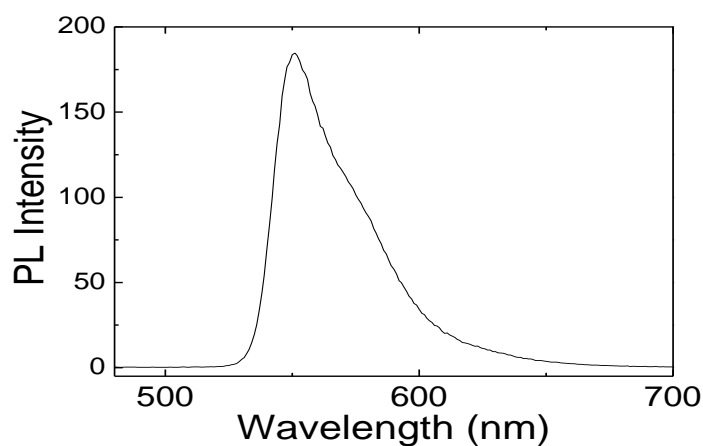


Figure 3.26. PL spectra of 1mM TTBC/PS(25 wt%) solution

TTBC/PS solution was electrospun at 10kV where TTBC concentration was 1mM and PS content was 25(wt)% in DMF. SEM images of resultant fibers are shown in Figure 3.27a. The structural analysis indicate that only H-aggregates were observed within TTBC/PS fibers (Figure 3.27b). It is concluded that the organic environment does not have significant effect on the formation of aggregates.

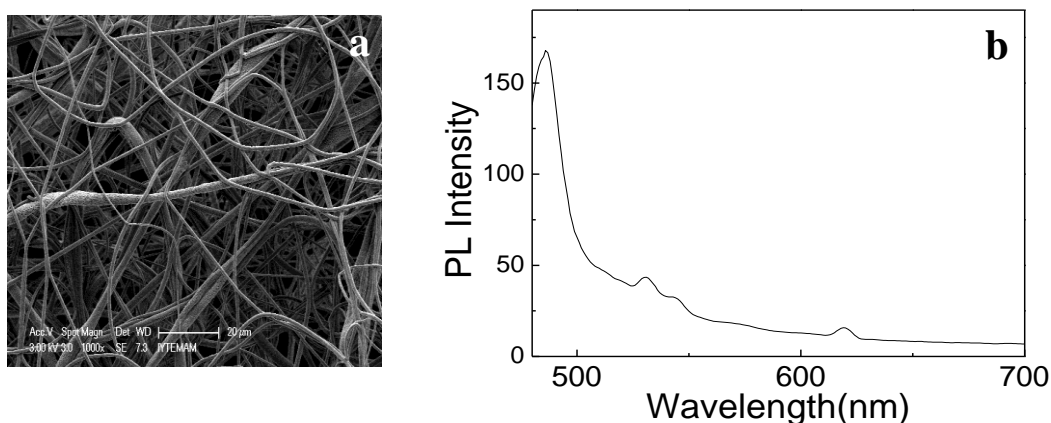


Figure 3.27. a) SEM image, b) PL spectra of TTBC/PS electrospun fibers

3.6. Pyrene Doped PS Fibers

Investigations on the effect of electrospinning on molecular aggregation was continued with another fluorescent molecule named **pyrene**. The molecular structure of pyrene given in Figure 3.28. Contrasting to cyanine type dyes, pyrene molecules can be aggregated into excimers. Excimers are dimers that formed through interactions of the excited states of two molecules. It is also frequently observed molecular self assembly process.

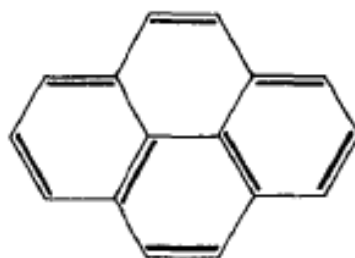


Figure 3.28. Molecular structure of Pyrene

The pyrene molecules dissolved in PS/DMF solution at concentrations ranging from 10^{-7} mM to 1 M. The precursor solutions were prepared at a wide concentration range so the pyrene solutions which had initially monomers or excimers were subjected to electrospinning process. The PL spectrum of Py/PS precursor solutions were given in Figure 3.29 (excitation wavelength was 317 nm). The monomer emission of pyrene molecules observed at 535 nm. For the concentrations of 0.1 mM to 1 M, the spectrum exhibit a strong band at 475 nm, which is attributed to the formation of excimers in solution (Stevens, et al. 1960).

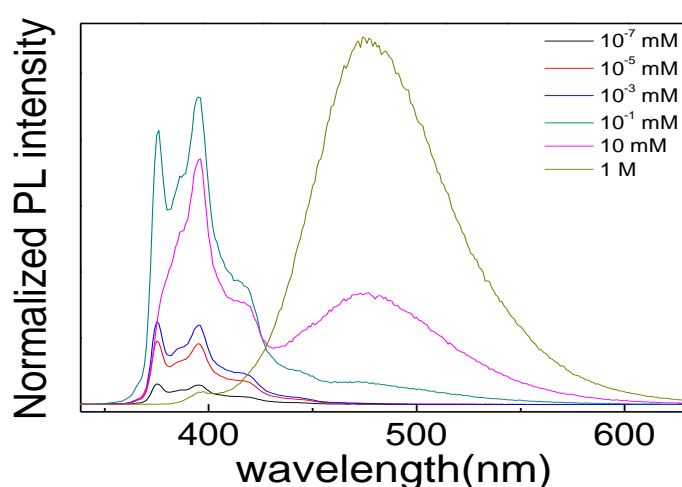


Figure 3.29. PL spectrum of Py/PS solutions at different [Py]

An aluminium foil was used as electrode in electrospinning rather than two parallel metal strips so only randomly deposited fibers were obtained. SEM images of the resultant fibers are shown in Figure 3.30. The fiber surface was found to be porous because of the capillary flow of polymer solution through the external boundary of charged liquid jet (Demir 2010). The diameter of the resulting fibers were about $2 \mu\text{m}$.

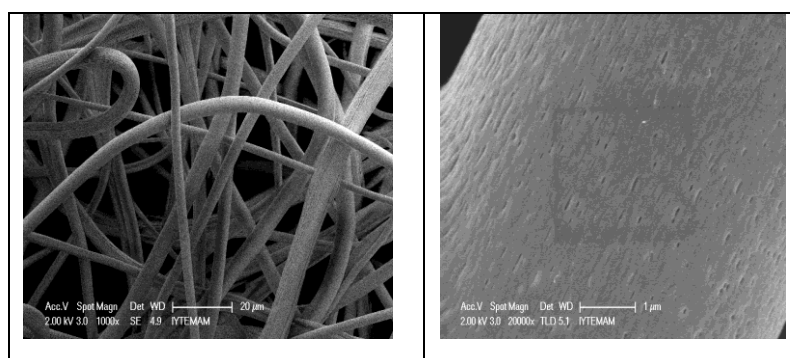


Figure 3.30. SEM Images of a) 10^{-3} mM pyrene doped 25 wt% PS fibers, b) PS fiber surface (magnification at 20,000 \times)

The PL spectrum of electrospun fibers are given in Figure 3.31a. However, the results showed that there were not any difference of pyrene molecules. The monomers in precursor solution were distributed into electrospun fibers as individual monomer molecules, not in excimer state. Only for 10mM Py/PS fibers has only monomers although the excimers were initially exist in solution. When the concentration increased to 1M, the excimers also observed within fibers similar to precursor solution of this concentration. In addition to electrospun fibers, spincoated and cast films were prepared. Similar results were observed in both types of films (Figure 3.31b and c). The method applied for film formation has no significant influence. As a result, it can be said that for specific concentrations of pyrene such as 10mM, electrospinning could be a method to get rid of excimers within fibers. The same effect observed for spincoated and cast films, as well.

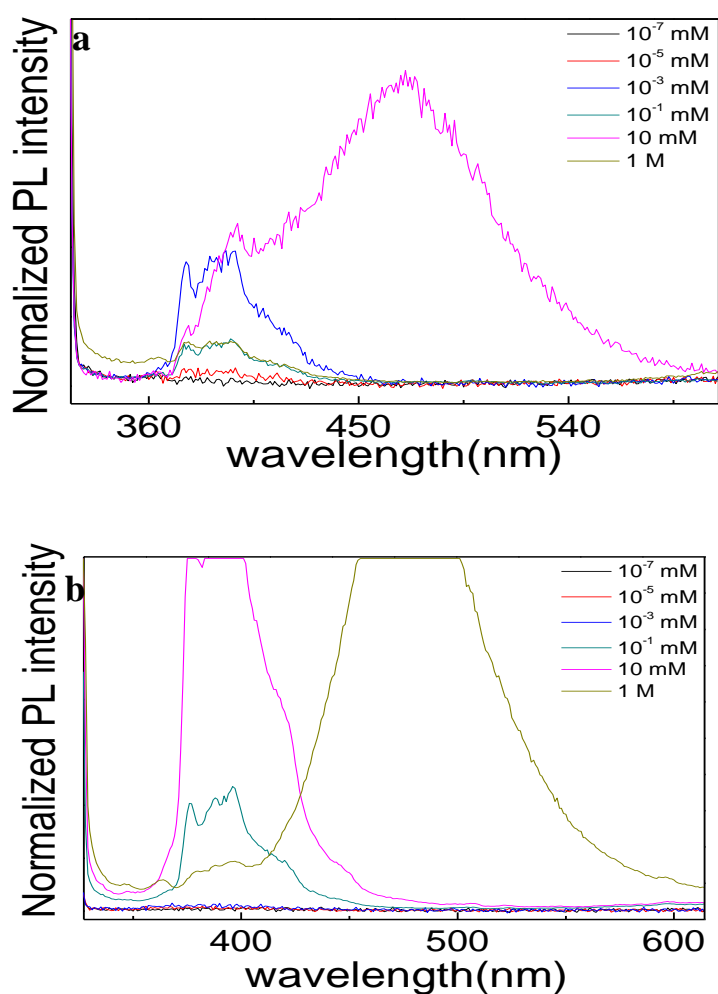


Figure 3.31. PL spectra of Py/PS a) electrospun fibers, b) spincoated, c) cast films

(cont. on next page)

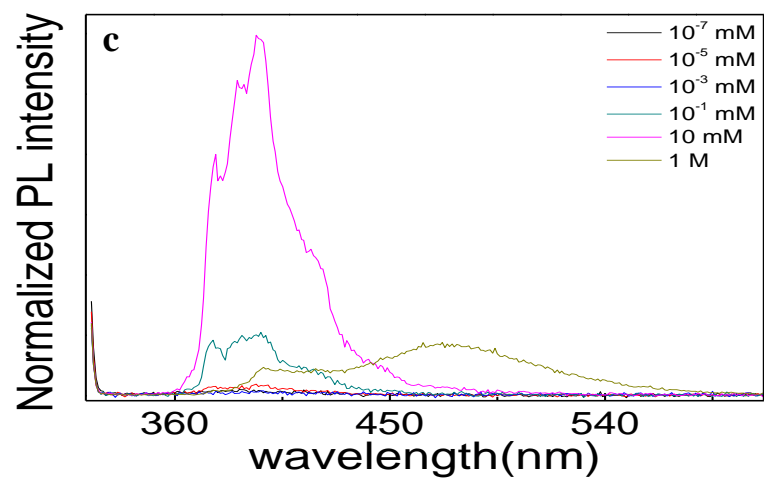


Figure 3.31. (cont.)

CHAPTER 4

CONCLUSION

Electrospinning process was applied to several pigment/polymer systems to investigate the effect of electrospinning on molecular aggregation of the pigments. The system that was analyzed more in detail was TTBC/PVA in aqueous solution. The solution and instrumental parameters of electrospinning were studied on this system but only H-aggregates of TTBC formed within PVA fibers. On the other hand, very well ordered structures were obtained for this system. There were three type of order at different length scales. First one was the alignment of fibers over mm^2 , second one was the orientation of PVA chains along the fiber axis and third one was the orientation of dye-aggregates of TTBC molecules within the fibers. Due to the orientation of H-aggregates was structural and highly polarized emission of the electrospun fibers was achieved. In addition, comparison of electrospinning with other thin film preparation techniques showed that electrospinning was found to be more efficient technique on the formation of H-aggregates of TTBC dye. Therefore, a self assembly process was successfully combined with electrospinning process. Other two systems employed here were TTBC/PS and Py/PS in DMF. For TTBC/PS system, H-aggregates of TTBC obtained within PS fibers that means the hydrophobicity of electrospinning has no direct influence on molecular aggregation of TTBC. For Py/PS system, no excimer formation was observed within fibers. However, for specific concentrations of Py, the excimers in solution were disintegrated by electrospinning process.

REFERENCES

- Baumgarten, P. (1971). "Electrostatic spinning of acrylic microfibers." *Journal of colloid and interface science* 36(1): 71-79.
- Bird, G. R., Zuckerman, B., Ames, A. E. (1968). *Photochem Phorobiol.* 8: 393.
- Birkan, B., D. Gülen, et al. (2006). "Controlled formation of the two-dimensional TTBC J-aggregates in an aqueous solution." *J. Phys. Chem. B* 110(22): 10805-10813.
- Chae, S., H. Park, et al. (2007). "Polydiacetylene supramolecules in electrospun microfibers: fabrication, micropatterning, and sensor applications." *Advanced Materials* 19(4): 521-524.
- Chen, Z., M. Foster, et al. (2001). "Structure of poly (ferrocenyldimethylsilane) in electrospun nanofibers." *Macromolecules* 34(18): 6156-6158.
- Deitzel, J., W. Kosik, et al. (2002). "Electrospinning of polymer nanofibers with specific surface chemistry." *Polymer* 43(3): 1025-1029.
- Demir, M., I. Yilgor, et al. (2002). "Electrospinning of polyurethane fibers." *Polymer* 43(11): 3303-3309.
- Demir, M. M. (2010). "Investigation on glassy skin formation of porous polystyrene fibers electrospun from DMF." *eXPRESS Polymer Letters* 4: 2-8.
- zen, et al. (2009). "Formation of Pseudoisocyanine J-Aggregates in Poly(vinyl alcohol) Fibers by Electrospinning." *The Journal of Physical Chemistry B* 113(34): 11568-11573.
- Demir, M. M., D. Soyol, et al. (2009). "Controlling Spontaneous Emission of CdSe Nanoparticles Dispersed in Electrospun Fibers of Polycarbonate Urethane." *The Journal of Physical Chemistry C* 113(26): 11273-11278.
- Dersch, R., T. Liu, et al. (2003). "Electrospun nanofibers: Internal structure and intrinsic orientation." *Journal of Polymer Science Part A: Polymer Chemistry* 41(4): 545-553.
- Dzenis, Y. (2004). "Material science: spinning continuous fibers for nanotechnology." *Science* 304(5679): 1917.
- Emerson, E. S., M. A. Conlin, et al. (1967). "The geometrical structure and absorption spectrum of a cyanine dye aggregate." *The Journal of Physical Chemistry* 71(8): 2396-2403.
- null
- Fidder, H. and D. Wiersma (1995). "Collective optical response of molecular aggregates." *Physica Status Solidi B Basic Research* 188: 285-285.

- Fong, H., I. Chun, et al. (1999). "Beaded nanofibers formed during electrospinning." *POLYMER-LONDON*- 40: 4585-4592.
- Huang, Z., Y. Zhang, et al. (2003). "A review on polymer nanofibers by electrospinning and their applications in nanocomposites." *Composites science and technology* 63(15): 2223-2253.
- James, T. H. and C. E. K. Mees (1977). *The Theory of the photographic process*. New York, Macmillan.
- Jones, R., L. Lu, et al. (2001). "Building highly sensitive dye assemblies for biosensing from molecular building blocks." *Proceedings of the National Academy of Sciences* 98(26): 14769.
- Kakade, M., S. Givens, et al. (2007). "Electric field induced orientation of polymer chains in macroscopically aligned electrospun polymer nanofibers." *Journal of the American Chemical Society* 129(10): 2777-2782.
- Kalra, V., P. Kakad, et al. (2006). "Self-assembled structures in electrospun poly (styrene-block-isoprene) fibers." *Macromolecules* 39(16): 5453-5457.
- Kameoka, J., R. Orth, et al. (2003). "A scanning tip electrospinning source for deposition of oriented nanofibres." *Nanotechnology* 14: 1124-1129.
- Katta, P., M. Alessandro, et al. (2004). "Continuous electrospinning of aligned polymer nanofibers onto a wire drum collector." *Nano Letters* 4(11): 2215-2218.
- Kim, G., A. Wutzler, et al. (2005). "One-dimensional arrangement of gold nanoparticles by electrospinning." *Chem. Mater* 17(20): 4949-4957.
- Kirstein, S. and S. Daehne (2006). "J-aggregates of amphiphilic cyanine dyes: Self-organization of artificial light harvesting complexes." *International Journal of Photoenergy* 8(5).
- Kobayashi, T. and K. Misawa (1997). "Hierarchical structure of one-dimensional J-aggregates." *Journal of Luminescence* 72-74: 38-40.
- Kodaira, T. and A. Amano (2007). *Optical information recording medium and method for producing the same*, Google Patents.
- Kuhn, H. B. (1970). *Chem. Phys. Lett.* 6: 183.
- Kuo, C.-C., Y.-C. Tung, et al. (2008). "Novel Luminescent Electrospun Fibers Prepared From Conjugated Rod-Coil Block Copolymer of Poly[2,7-(9,9-dihexylfluorene)]-*block*-Poly(methyl methacrylate)." *Macromolecular Rapid Communications* 29(21): 1711-1715.
- Li, D., Y. Wang, et al. (2003). "Electrospinning of polymeric and ceramic nanofibers as uniaxially aligned arrays." *Nano Letters* 3(8): 1167-1171.

- Moliton, A. and R. Hiorns (2004). "Review of electronic and optical properties of semiconducting -conjugated polymers: applications in optoelectronics." *Polymer International* 53(10): 1397-1412.
- Moon, S., J. Choi, et al. (2008). "Preparation of aligned polyetherimide fiber by electrospinning." *Journal of Applied Polymer Science* 109(2): 691-694.
- Naber, A., U. Fischer, et al. (1999). "Architecture and surface properties of monomolecular films of a cyanine dye and their light-induced modification." *J. Phys. Chem. B* 103(14): 2709-2717.
- O'brien, D. F. (1974). *Phorogr. Sci. Eng.* 18: 16.
- Okamoto, K., P. Chithra, et al. (2009). "Self-Assembly of Optical Molecules with Supramolecular Concepts." *International Journal of Molecular Sciences* 10(5): 1950.
- Palmer, L. and S. Stupp (2008). "Molecular Self-Assembly into One-Dimensional Nanostructures." *Accounts of Chemical Research* 41(12): 1674-1684.
- Platt, J. (1956). *J. Chem. Phys.* 25: 80-105.
- Reneker, D. and I. Chun (1996). "Nanometre diameter fibres of polymer, produced by electrospinning." *Nanotechnology* 7: 216-223.
- Reneker, D., A. Yarin, et al. (2000). "Bending instability of electrically charged liquid jets of polymer solutions in electrospinning." *Journal of Applied Physics* 87: 4531.
- Stevens, B. and E. Hutton (1960). "Radiative Life-time of the Pyrene Dimer and the Possible Role of Excited Dimers in Energy Transfer Processes."
- Sundaray, B., V. Subramanian, et al. (2004). "Electrospinning of continuous aligned polymer fibers." *Applied physics letters* 84: 1222.
- Tani, T. (1996). "J-aggregates in spectral sensitization of photographic materials." *J-aggregates*: 209.
- Taylor, G. (1964). "Disintegration of Water Drops in an Electric Field." *Proceedings of the Royal Society of London. Series A. Mathematical and Physical Sciences* 280(1382): 383-397.
- Theron, A., E. Zussman, et al. (2001). "Electrostatic field-assisted alignment of electrospun nanofibres." *Nanotechnology* 12: 384.
- Whitesides, G. and B. Grzybowski (1994). Self-assembly at all scales.
- Whitesides, G. M. and B. Grzybowski (2002). "Self-Assembly at All Scales." *Science* 295(5564): 2418-2421.

- Yamamoto, Y. and R. Slusher (1993). "Optical processes in microcavities." *Physics Today* 46: 66-73.
- Yang, F., R. Murugan, et al. (2005). "Electrospinning of nano/micro scale poly (L-lactic acid) aligned fibers and their potential in neural tissue engineering." *Biomaterials* 26(15): 2603-2610.
- Yao, H., S. Sugiyama, et al. (1999). "Spectroscopic and AFM studies on the structures of pseudoisocyanine J aggregates at a mica/water interface." *J. Phys. Chem. B* 103(21): 4452-4456.